Coordination Chemistry Reviews 254 (2010) 309–330

Contents lists available at ScienceDirect

Coordination Chemistry Reviews

journal homepage: www.elsevier.com/locate/ccr

Review

Ruthenium complexes with non-innocent ligands: Electron distribution and implications for catalysis

Julie L. Boyer, Jonathan Rochford, Ming-Kang Tsai, James T. Muckerman, Etsuko Fujita*

Chemistry Department, Brookhaven National Laboratory, BLDG 555, Upton, NY 11973-5000, United States

Contents

ARTICLE INFO

Article history:
Received 5 May 2009
Accepted 6 September 2009
Available online 11 September 2009

Keywords:
Ruthenium complexes
Redox-active ligands
Non-innocent ligands
Quinone
Oxidation
Catalysis

ABSTRACT

Ruthenium complexes with the non-innocent ligands (NILs) benzoquinone, iminobenzoquinone and benzoquinonediimine and their redox derivatives exhibit intriguing electronic properties. With the proper ligand set the NIL π* orbitals mix extensively with the ruthenium dπ orbitals resulting in delocalized electron distributions and non-integer oxidation states, and in most of these systems a particular ruthenium oxidation state dominates. This review critically examines the electronic structure of Ru–NIL systems from both an experimental and computational (DFT) perspective. The electron distribution within these complexes can be modulated by altering both the ancillary ligands and the NIL, and in a few cases the resultant electron distributions are exploited for catalysis. The Ru–NIL systems that perform alcohol oxidation and water oxidation catalysis are discussed in detail. The Tanaka catalyst, an anthracene-bridged dinuclear Ru complex, is an intriguing example of a Ru–NIL framework in catalysis. Unlike other known ruthenium water oxidation catalysts, the two Ru atoms remain low valent during the catalytic cycle according to DFT calculations, some experimental evidence, and predictions based on the behavior of the related mononuclear species.

Abbreviations: bbp, 2,6-bis(benzimidazol-2-yl)pyridine; btpyxa, 2,7-di-tert-butyl-9,9-dimethyl-4,5-bis(2,2′:-6′,2″-terpyrid-4′-yl)xanthene); btpyan, 1,8-bis(2,2′:6′,2″-terpyridyl)anthracene; dppb, 1,4-bis(diphenylphosphine)butane; edta, ethylenediaminetetraacetic acid; NH_2–L, bis(2-pyridylmethyl)-2-aminoethylamine; NPh–bpa, 2-(bis(2-pyridylmethyl)aminomethyl)anilido ligand; Me_3tacn, 1,4,7-trimethyl-1,4,7-triazacyclononane; TBA, tertrabutylammonium; TFA, trifluoroacetate; V_{rest}, rest potential.

* Corresponding author. Tel.: +1 631 344 4356.
E-mail address: fujita@bnl.gov (E. Fujita).

0010-8545/$ – see front matter © 2009 Elsevier B.V. All rights reserved.
doi:10.1016/j.ccr.2009.09.006

1. Introduction

Metal-based radicals and redox transformations are the cornerstones of most catalytic cycles. Growing in importance – yet still underutilized – are metal complexes with redox addressable co-ligands that catalyze chemical reactions [1–7]. Nature, however, often exploits redox-active organics in chemical transformations [8]. Amine oxidase and galactose oxidase are two prominent examples of redox-active organic groups and metal centers working cooperatively in catalysis [2,9].

Studies on alternative energy sources are of irrefutable environmental and economic importance [10]. Water is an attractive feedstock for renewable fuels. The oxidation of two water molecules generates four electrons in addition to four protons and molecular oxygen (Eq. (1)). This deceivingly simple conversion, however, has a potential of $E^{\circ} = 0.82$ V *vs.* NHE at pH 7 and requires a catalyst in addition to an applied overpotential. In photosystem II, a nearby redox-active tyrosine residue ($^{\bullet}OTyr_z$) relays the necessary oxidizing equivalents to the manganese-containing cluster. This is coupled with a proton transfer from a nearby histidine [11–18]. A variety of dinuclear coordination compounds catalyze the oxidation of water, but most systems are plagued by poor to modest turnover numbers [19,20]. The Tanaka catalyst ($[Ru_2(btpyan)(3,6\text{-}^tBu_2C_6H_2O_2)_2(OH)_2]^{2+}$ where btpyan = 1,8-bis(2,2′:6′,2″-terpyridyl)anthracene) exhibits excellent activity for water oxidation [21–23]. The Tanaka catalyst is unique in its employment of redox-active dioxolene ligands, and it is these redox-active ligands that underpin the extraordinary reactivity of this complex.

$$2H_2O \rightarrow O_2 + 4H^+ + 4e^- \quad (1)$$

Non-innocent ligands comprised of 1,2 disubstituted phenylene redox-active subunits (Scheme 1), henceforth denoted NIL, have been increasingly studied since the 1970s due to their intriguing electronic properties [24–30]. These bidentate ligands have three oxidation states (NIL^{Red}, $NIL^{\bullet}$ and NIL^{Ox})[1] related by one-electron redox transformations (Scheme 1). The combination of NILs with redox-active transition metals can afford redox tautomers, complexes related by the intramolecular transfer of an electron between the NIL and metal fragments [30,31]. For example, upon the application of an external stimulus such as temperature, the complex $[Co^{III}(NIL^{Red})(NIL^{\bullet})(bpy)]$ transfers an electron from the NIL^{Red} to the Co center to form $[Co^{II}(NIL^{\bullet})_2(bpy)]$. Whereas the valence tautomers $[Co^{III}(NIL^{Red})(NIL^{\bullet})(bpy)]$ and $[Co^{II}(NIL^{\bullet})_2(bpy)]$ are complexes of distinct and different localized electron distributions, complexes with a single delocalized electron distribution (i.e., non-integer oxidation state) can also occur in M-NIL systems. Ambiguous or non-integer oxidation state assignments of the metal and NIL fragments occur when there is a large degree of mixing between the metal and NIL orbitals [32]. The extent of delocalization is determined by the energies of the frontier orbitals (inclusive of symmetry and overlap) of the NIL and metal. Such delocalized electron distributions are prevalent in Ru–NIL chemistry [33].

The possible oxidation states for the Ru–NIL systems and their spin multiplicities are depicted in Scheme 2. The oxidation-state assignments within these resonance structures are intrinsically a valence-bond (VB) concept because the active electrons are assigned to the localized metal and/or ligand orbitals. Owing to extensive mixing of the Ru(dπ) and NIL(π*) orbitals, the electronic state in a complex may have contributions from multiple resonance forms. Moreover, it is important not only to distinguish between electronic configurations in the (delocalized) molecular orbital (MO) picture and those in the (localized) VB picture, but to understand how electronic configurations of states in the MO picture map onto those in the VB picture. Details of the VB and MO pictures of the bonding in Class B complexes and their interrelationship are provided in Appendix. In the resonance forms in Scheme 2, we are assigning up to two electrons to two localized orbitals in various ways, yet most electronic structure calculations are based on configurations in the delocalized molecular orbitals. Class A, Class B and Class C redox states all contain at least two resonance forms, whereas Class D describes the unambiguous closed-shell singlet electron distribution Ru^{II}–NIL^{Red}. Class A species, although electron deficient, can be stabilized by an appropriate choice of co-ligand [34–38]. In the VB picture, three resonance structures correspond to the problematic Class B singlet states; two closed-shell states (Ru^{II}–NIL^{Ox} and Ru^{IV}–NIL^{Red}) and one open-shell state (Ru^{III}–$NIL^{\bullet}$). The electronic configuration giving rise to the open-shell singlet Ru^{III}–$NIL^{\bullet}$ species can also lead to an open-shell triplet species, which has no resonance stabilization owing to spin restrictions. There are also conceivable cases where nearly degenerate singlet and triplet states could be mixed by spin-orbit coupling arising from the heavy Ru center. The Class B open-shell "anti-ferromagnetically coupled" singlet state refers to the VB open-shell singlet resonance state, which cannot be expressed in terms of a single electronic configuration when electron spin is taken into account; it is not enough to specify that the two electrons are in different localized fragment orbitals, one has to specify how their spins are coupled. Ironically, but rigorous algebraically, the proper description of this anti-ferromagnetically coupled open-shell singlet state in the (delocalized) MO picture involves only two closed-shell configurations: the closed-shell singlet ground-state configuration and the configuration generated by promotion of the *pair* of electrons in the π HOMO of the closed-shell ground-state singlet configuration to the corresponding π* LUMO in a manner known as a generalized valence-bond configuration interaction (GVB-CI). The open-shell MO singlet state is energetically less favorable than the lower lying ferromagnetically coupled triplet configuration [39], but the VB open-shell singlet state can be a strong participant in the resonance stabilization of the singlet ground state of a system through interaction with the non-orthogonal VB Class B closed-shell Ru^{II}–NIL^{Ox} and Ru^{IV}–NIL^{Red} singlet states. It is possible that in systems of reduced overlap and minimal delocalization across the metal–NIL framework, the VB open-shell Class B singlet state may actually be the dominant contributor to the (multiconfigurational) ground singlet state. Sometimes calculations that neglect this resonance interaction incorrectly predict the Class B triplet state (since there is only one triplet state, it is the same state in both the VB and MO pictures) to be the electronic ground state of the system [39]. There have been numerous reports in the literature of Class B anti-ferromagnetically coupled Ru^{III}–$NIL^{\bullet}$ species, however, these assignments are often ambiguous and reflect intermediate cases that contain substantial (if not predominant) Ru^{II}–NIL^{Ox} character [39,40]. The Class C systems are typically less ambiguous than Class B even though there exist two possible resonance forms (both of doublet multiplicity). The Class C Ru^{II}–$NIL^{\bullet}$ is usually predominant, however, by careful choice of ligand set the Ru^{III}–NIL^{Red} resonance form can dominate [41,42].

This review examines the electronic structure of Ru–NIL systems and the potential to modulate the electron distribution within these complexes by altering both the ancillary ligands and the NIL. Although the majority of complexes discussed here are studied from a fundamental characterization point of view, these studies are essential to understanding the few Ru–NIL systems that are

[1] As $NIL^{\bullet}$ can be formed by either oxidatively or reductively, it can be interpreted as a cationic or anionic radical depending whether the precursor is NIL^{Red} or NIL^{Ox}, respectively. For the purpose of this review we use the term $NIL^{\bullet}$ generically without implying the redox process involved in its generation.

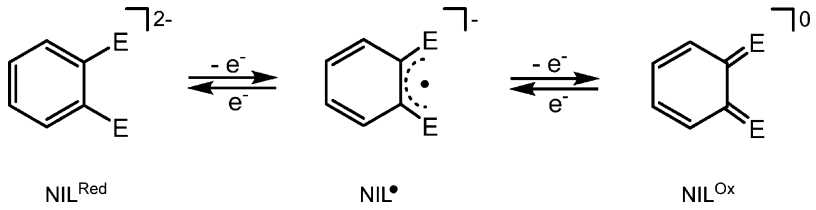

Scheme 1. Redox transformations for NIL ligands where E = O or NR, or a combination of these heteroatoms.

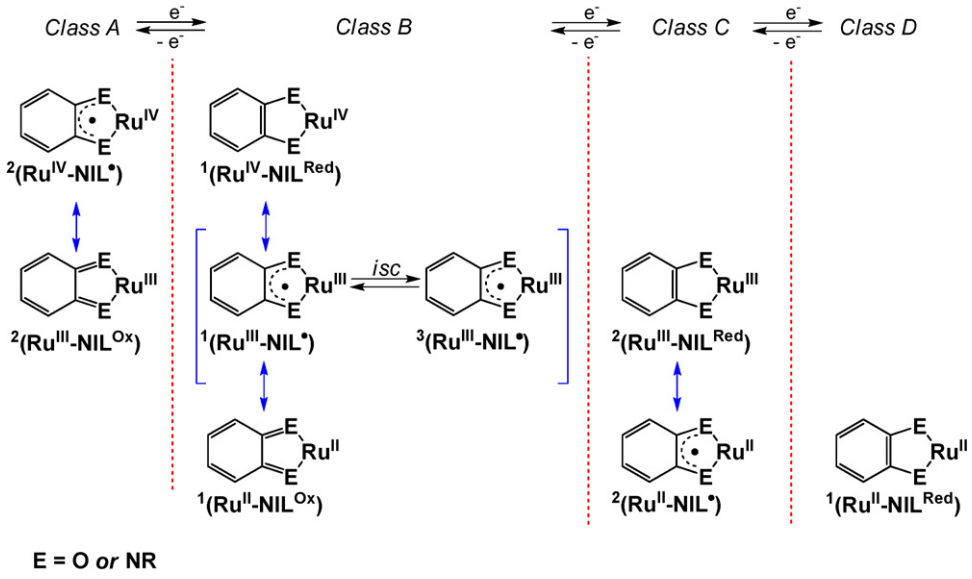

Scheme 2. Oxidation states in the various resonance structures for Ru–NIL type complexes. The various redox states have been divided into four classes. Spin multiplicities are indicated as leading superscripts in the oxidation state designations (For Class B systems, resonance is only spin-allowed for the singlet states. Formation of a Class B system, via reduction of a Class A species or oxidation of a Class C species, can result in the singlet or triplet open-shell states depending on the co-ligands involved.), and possible intersystem crossing between singlet and triplet states is indicated by "isc".

active components in catalytic cycles. In an effort to remain concise, this review is focused on systems containing one non-bridging NIL per ruthenium center. For discussions of multi-metallic and/or multi-NIL systems the reader is referred to the relevant literature [43–53].

2. Characterization

Determining the electron distribution in Ru–NIL complexes is often non-trivial and entails a variety of experimental and theoretical studies performed in concert. Identification of the electronic structure of Class B systems is especially challenging due to complications in distinguishing between open- and closed-shell forms which involve spin-multiplicity constraints [39]. Identification of the contributing electronic configuration in a system containing a single paramagnetic center (Class C) is generally less complicated. A variety of spectroscopic measurements such as UV–vis, EPR, XPS, IR, Raman, along with electrochemical experiments and X-ray crystallography studies can assist in elucidating the electron distribution within a given system [54,55].

2.1. X-ray crystallography

The C–C and C–E distances within the NIL are often employed as a diagnostic tool for determining the NIL's oxidation state. Bhattacharya et al. proposed the following table of bond lengths (±0.01 Å) for the three oxidation states of the NIL (Table 1) [56]. In ruthenium chemistry, however, the use of X-ray crystallography as the sole method of determining electron distribution can often lead to an erroneous assignment.[2]

Table 1
Average bond lengths (Å) for NIL.

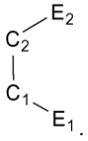

	C–E		C_1–C_2
	E = O	E = NR	
NIL^{Ox}	1.22	1.31	1.48
NIL•	1.30	1.35	1.43
NIL^{Red}	1.34	1.38	1.42

2.2. Electrochemistry and electronic spectroscopy

The energy of the lowest spin-allowed MLCT transition of a transition-metal complex can be related to the standard potential by the relationship $h\nu_{MLCT} = \Delta E'_{Redox} + R$ (expressed in eV, where '*R*' represents the sum of a number of reorganization energies and various solvation terms). The value of *R* is typ-

[2] These averaged data are obviously influenced by the non-innocence of these ligands, showing a longer C_1–C_2 bond length in NIL^{Red} than is expected for an aromatic system (1.38–1.40 Å). Also, Wieghardt cites shorter C_1–C_2 distance for the phenylenediamine ligand of 1.40 Å [57].

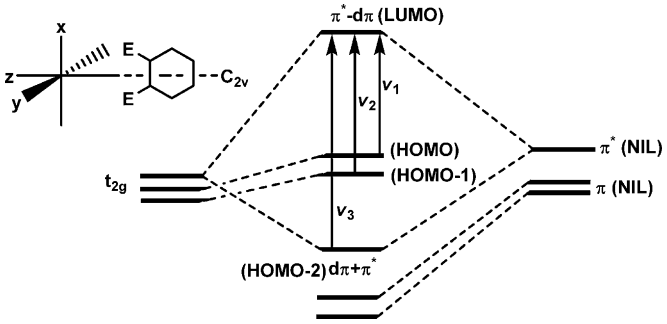

Fig. 1. Frontier molecular orbitals of Ru–NIL systems.

ically on the order of *ca.* 0.2–0.4 eV [58–60]. The HOMO-1 or HOMO-2 orbitals may be involved in the optical transition (as opposed to the HOMO for E_{ox}), however, the energy difference is usually within that of '*R*'. Ruthenium polypyridyl complexes typically display $h\nu_{MLCT} - \Delta E'_{Redox}$ differences of *ca.* 0.2 eV (i.e., within the approximated reorganization energy '*R*').[3] Class B Ru–NIL systems deviate from this type behavior [61]. For example, the complex $[Ru(C_6H_4NHNH)(bpy)_2]^{2+}$ has a $h\nu_{MLCT} - \Delta E'_{Redox}$ difference of 0.59 eV emphasizing its departure from the simplistic valence bond MLCT picture [62]. The occurrence of extensive Ru(dπ)–NIL(π*) mixing in Class B Ru–NIL species is usually characterized by intense low-energy bands that appear to have little charge transfer character, i.e., they only show weak solvatochromism, and whose resonance Raman spectra show enhancement of only one metal–ligand vibration [25,33,62–64]. Such complexes are also known to show parallel slopes for Hammett plots of their first oxidation and reduction potentials [25,65]. Collectively this behavior suggests a highly delocalized Ru–NIL structure due to extensive mixing of the Ru(dπ) and NIL(π*) orbitals with substantial contributions of both the (non-orthogonal) Ru^{II}–NIL^{Ox} and Ru^{III}–NIL• resonance forms. These intense absorptions have been described as ML → ML transitions[4] consistent with their large exchange integrals (*ca.* 7000 cm^{-1}) which are closer to that of a ligand based π–π* transition (8000–11 000 cm^{-1}) than a pure d–π* MLCT transition (<1000 cm^{-1}) [25,33,55,59,62].

The electronic spectra and redox chemistry of Ru–NIL complexes can be explained by a simple molecular orbital diagram as shown in Fig. 1 (coordinates are adopted from Ref. [2] where the bonding t_{2g} metal orbitals are classified as d_{XY}, d_{YZ} and $d_{X^2-Z^2}$) [25,62,66]. Of greatest interest are the molecular orbitals derived from the Ru(t_{2g}), NIL(π) and NIL(π*) sets of orbitals, in particular the HOMO, HOMO-1, HOMO-2 and LUMO orbitals, as these are responsible for the bands observed in the UV–vis-NIR regions of the spectrum. The relative energies of these orbitals will determine the extent of ruthenium and NIL mixing and thus govern the electronic properties of these systems. At this point it is important to note that an understanding of the frontier orbitals of such complexes will give a better understanding of their reactivity. The filled Ru(t_{2g}) set of orbitals (d_{XY}, d_{YZ} and $d_{X^2-Z^2}$) is split by interactions with both the NIL(π) and NIL(π*) orbitals. Two of the Ru(t_{2g}) orbitals (d_{XY} and $d_{X^2-Z^2}$) are destabilized by the filled NIL(π) orbital and can give rise to two low energy, HOMO → LUMO and (HOMO-1) → LUMO MLCT transitions (ν_1 and ν_2 in Fig. 1, respectively). Note, however, these transitions are only possible when the ligand is in the NIL^{Ox} (empty) or NIL• (partially filled) oxidation state. Energy and symmetry permitting, the co-ligand orbitals may also contribute to the HOMO orbital, e.g., for $[Ru(trpy)(NIL)(X)]^{n+}$ there is a significant contribution to the HOMO from the ligand X that increases with Lewis basicity where $X = OH_2 < OH^- < O^{2-}$ [39]. The remaining Ru(t_{2g}) orbital, d_{YZ}, is stabilized by strong overlap with the NIL(π*) orbital giving rise to the (HOMO-2) → LUMO transition (ν_3 in Fig. 1), again for NIL^{Ox} and NIL• redox states only.[5] Due to the strong overlap of the molecular orbitals which give rise to the (HOMO-2) → LUMO transition, this absorption typically dominates the UV–vis spectra of this class of compounds, and can be described as a MLCT transition.[4]

Importantly, for a Class B system [cf., Scheme 2] the degree of mixing between the HOMO-2 and LUMO orbitals will, to a large extent, determine how much Ru^{III}–NIL• resonance character this system will possess (of course, the co-ligands on the metal and any substituents on the NIL will play a role in determining the energies of these orbitals). For many Class B systems, a combination of experimental and theoretical methods have failed to give a clear, unambiguous assignment of the localized oxidation states of the metal and NIL fragments. In these cases, however, the Ru(π)–NIL(π*) systems are so highly delocalized that neither of the charge-localized representations adequately conveys the true electronic structure, although one may show predominance over the other. It is therefore very difficult to assign definitive localized oxidation states for these Class B systems.

3. Synthesis

Redox reactions are ubiquitous in the preparation of M–NIL complexes (Scheme 3). The oxidative substitution of benzoquinones to metal carbonyls is extensively utilized in M–NIL chemistry [67]. Balch provides an excellent example of this preparative method within Ru–NIL chemistry [68]. The treatment of $Ru(CO)_3(PPh_3)_2$ with tetrachloroquinone affords the complex $Ru^{II}(Cl_4C_6O_2)(CO)_2(PPh_3)_2$ with the NIL in the catecholate oxidation state. Alternatively, $Ru^{II}(Cl_4C_6O_2)(CO)_2(PPh_3)_2$ can be prepared by metathesis via the treatment of $Ru(CO)_2(PPh_3)_2Cl_2$ with deprotonated tetrachlorocatechol. The preparation of benzoquinonediimine by the oxidative dimerization of two aniline ligands represents an unconventional route to M–NIL systems [69–72]. The ruthenium center plays dual roles in the coupling reaction, it coordinates the two anilino ligands placing them in close proximity and it supplies some of the necessary oxidizing equivalents for the coupling. This method is implemented in the preparation of $Ru(C_6H_4NHNPh)(acac)_2$, synthesized from $Ru(acac)_3$ refluxed in neat aniline in air [70].

Redox reactions between the NIL and an ancillary ligand are established in Ru–NIL chemistry. For example, treatment of the metal hydride $Ru(CO)(PPh_3)_3HCl$ with 3,5-di-*tert*-butylquinone affords $Ru(3,5\text{-}^tBu_2C_6H_2O_2)(Cl)(CO)(PPh_3)_2$ along with the generation of 1/2 equiv of hydrogen gas [73]. The reduction of the quinone to the semiquinone state is coupled with the formation of H_2. This is an intriguing example which highlights the potential Ru–NIL complexes have for interacting with important substrates, even if only stoichiometrically.

[3] Strickly speaking, this equation is dimensionally incorrect because it should be the free energies associated with the one-electron redox process, not the redox potentials, that are compared to the MLCT transition energy. Since $\Delta G^\circ_{Redox} = -F\Delta E^\circ_{Redox}$, the equation should be $h\nu_{MLCT} = -F(E^\circ_{Red} - E^\circ_{Ox}) + R$ (where *F* is Faraday's constant), but we will follow tradition in this review.

[4] The CT nature of this transition will vary greatly depending on the ligand set in the complex. For the purpose of this review, the term MLCT is used, however, in some cases this transition may be better described as ML → ML [25,33,55,59,62].

[5] This is a very basic representation of the Ru-NIL interaction where splitting of the t_{2g} levels by ancillary ligands is neglected. The relative energies of the HOMO and HOMO-2 orbitals can be reversed depending on the level of theory used [33].

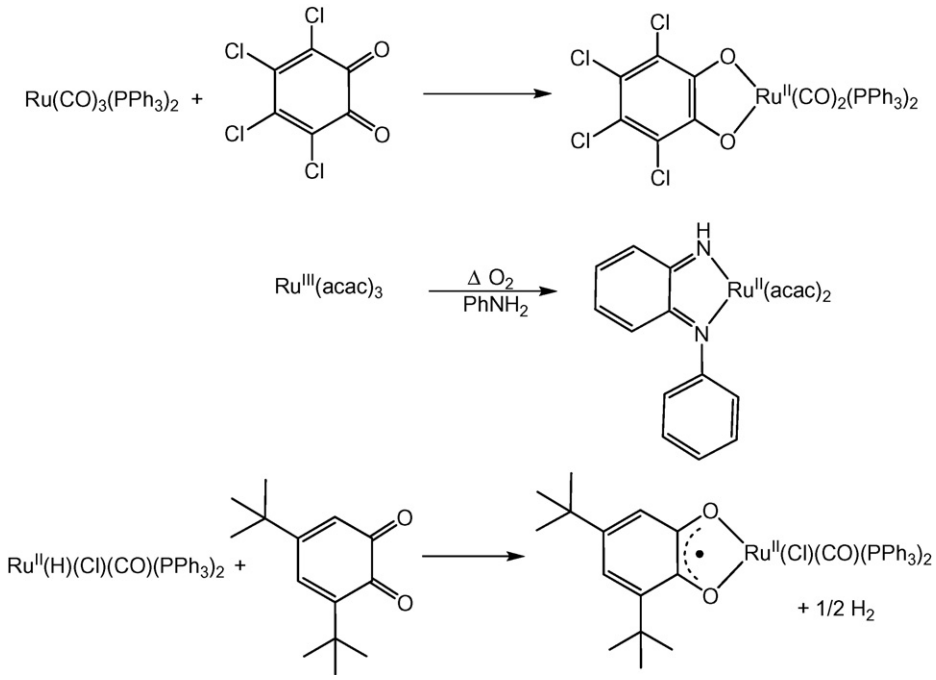

Scheme 3. Redox reactions in the preparation of Ru–NIL complexes.

4. $Ru(NIL)L_2L'_2$

4.1. L = phosphine, L′ = hydride

The majority of the complexes discussed in this review display significant electron delocalization over the Ru and NIL fragments, however, it is important to note that with a judicious choice of co-ligands, localized electron distributions are attainable. The complex $Ru(C_6H_4O_2)(P^iPr_3)_2(H)_2$ displays the longest C–O distances (1.350(6) and 1.348(6) Å) and the shortest C_1–C_2 distance (1.406(6) Å) tabulated in this review (Table 2) [74]. These values are consistent with the catecholate ligand oxidation state, and the complex is assigned Ru^{IV}–NIL^{Red}. Our preliminary DFT calculations support the ground state assignment of Ru^{IV}–NIL^{Red} with the Ru^{III}–$NIL^{\bullet}$ and Ru^{II}–NIL^{Ox} states higher in energy [75]. The complex $Ru(C_6H_4O_2)(P^iPr_3)_2(H)_2$ exhibits a distorted octahedral geometry and the contribution from a single Class B electronic state is likely due to minimal overlap between NIL(π^*) and the Ru(t_{2g}) orbitals (Fig. 2) [76].

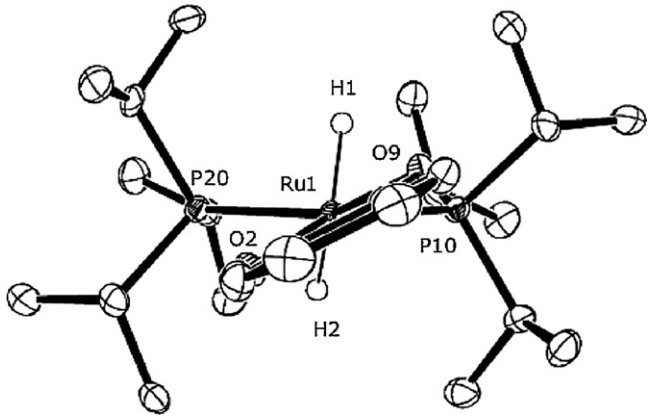

Fig. 2. Molecular structure of $Ru(C_6H_4O_2)(P^iPr_3)_2(H)_2$ omitting for clarity the hydrogen atoms attached to carbon atoms. This figure was reproduced from Ref. [74] with permission of the copyright holders.

Treatment of $Ru^{IV}(C_6H_4O_2)(P^iPr_3)_2(H)_2$ with CO liberates H_2 concomitant with formation of the $Ru^{II}(C_6H_4O_2)(P^iPr_3)_2(CO)_2$. The amidophenolate analog $Ru(C_6H_4ONH)(P^iPr_3)_2(H)_2$ heterolytically cleaves H_2 to form $Ru(C_6H_4ONH_2)(P^iPr_3)_2(H)_3$. The species $Ru(C_6H_4ONH)(P^iPr_3)_2(H)_2$ catalytically hydrogenates olefins in the presence of H_2. Although these complexes display reactivity with interesting substrates, the NIL functions only as a redox *in*active co-ligand [74].

Class D complexes are generally considered to have the unambiguous electron distribution of Ru^{II}–NIL^{Red} with contributions from the Ru^{I}–$NIL^{\bullet}$ and Ru^{0}–NIL^{Ox} resonance forms unlikely. Examples of Class D complexes include $Ru(C_6H_4O_2)(PMe_3)_4$, $Ru(C_6H_4NHNH)(PPh_3)_3$, $(NEt_4)[Ru(Cl_4C_6O_2)(CN)(CO)_2(PPh_3)]$, $Ru(C_6H_4O_2)(PPh_3)_2(CO)_2$, and $Ru(Br_4C_6O_2)(PPh_3)_2(CO)_2$ [77–80].

4.2. L′ = carbonyl

The pioneering work by Balch provides an excellent example of ligand localized redox transformations [68]. Treatment of the complex $Ru(Br_4C_6O_2)(PPh_3)_2(CO)_2$ with the oxidant $AgPF_6$ affords $[Ru(Br_4C_6O_2)(PPh_3)_2(CO)_2]PF_6$ (Scheme 4). The IR spectrum of $[Ru(Br_4C_6O_2)(PPh_3)_2(CO)_2]PF_6$ features CO bands at 2074 and 2023 cm^{-1}, shifted from 2046 and 1994 cm^{-1} in the neutral precursor. This small shift in CO frequency is consistent with a ligand-based oxidation [81,82]. The EPR spectrum of $[Ru(Br_4C_6O_2)(PPh_3)_2(CO)_2]PF_6$ displays little anisotropy at 77 K with $g_{\perp}$ and $g_{||}$ values of 2.02 and 2.00, respectively (Table 3). Collectively, the data is consistent with a Ru^{II}–$NIL^{\bullet}$ assignment for the oxidized species. The ligand-based redox reactivity is reversible; reduction of $[Ru^{II}(NIL^{\bullet})(PPh_3)_2(CO)_2]PF_6$ with zinc dust regenerates the $Ru^{II}(NIL^{Red})(PPh_3)_2(CO)_2$ complex.

4.3. L′ = chloride

The isostructural Class B complexes $Ru(NIL)(PPh_3)_2Cl_2$ (NIL = 3,5-$^tBu_2C_6H_2O_2$, C_6H_4ONH, and C_6H_4NHNH) have been reported [56,83,84]. The coordination sphere of the $Ru(NIL)(PPh_3)_2Cl_2$ complexes contains two Cl ligands and a

Table 2
Selected bond distances (Å) in Ru–NIL complexes.

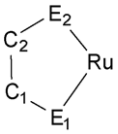

Complex	Ru–E_1	Ru–E_2	C_1–E_1	C_2–E_2	C_1–C_2	Ref.
Class B						
$Ru(C_6H_4O_2)(P^iPr_3)_2(H)_2$	2.027(3)	2.031(3)	1.348(6)	1.350(6)	1.406(6)	[74]
$Ru(3,5\text{-}^tBu_2C_6H_2O_2)(PPh_3)_2Cl_2$	1.995(3)	2.071(3)	1.298(6)	1.305(6)	1.432(6)	[83]
$Ru(C_6H_4ONH)(PPh_3)_2Cl_2$[a]	2.003(2)		1.308(4)		1.431(7)	[56]
$Ru(C_6H_4ONH)(acac)_2$	2.0452	1.9063	1.2914	1.3404	1.439	[34]
$Ru(C_6H_4NHNH)(dppb)Cl_2$	2.103(2)	2.056(3)	1.349(4)	1.351(4)	1.436(4)	[112]
$Ru(C_6H_4NHNH)(PPh_3)_2Cl_2$	1.979(3)	1.974(3)	1.322(4)	1.318(4)	1.431(5)	[84]
$Ru(C_6H_4NHNH)(NH_3)_2Cl_2$[a]	1.969(3)		1.330(5)		1.457(7)	[113]
$Ru(C_6H_4NHNH)(acac)_2$[a]	1.958(2)		1.320(3)		1.450(5)	[114]
$Ru(C_6H_4NHNPh)(acac)_2$	1.958(5)	1.996(5)	1.333(8)	1.352(8)	1.441(9)	[70]
$Ru(C_6H_4NHNPh)(NH_2Ph)_2Cl_2$	1.940(4)	1.997(4)	1.319(7)	1.343(7)	1.440[c]	[70]
$[Ru(C_6H_4NHNH)(PPh_3)_2(NCMe)_2](PF_6)_2$[a]	2.011(3)		1.308(4)		1.457(5)	[115]
$[Ru(C_6H_4NHNH)(Me_3tacn)(OH_2)](PF_6)_2$[a]	1.998(3)		1.314(4)		1.446(7)	[116]
$[Ru(C_6H_4NHNH)(Me_3tacn)I](PF_6)$[a]	1.991(3)		1.318(5)		1.445(8)	[116]
$[Ru(C_6H_4NHNH)(Me_3tacn)(N_3)](PF_6)$	1.983(4)	1.991(4)	1.320(6)	1.321(6)	1.448(7)	[116]
$[Ru((C_6H_4NHNH)(PPh_3)(CO)_2Br)Br$	2.07(2)	2.08(2)	1.26(2)	1.29(2)	1.51(2)	[117]
$[Ru(C_6H_4NHNH)(bpy)_2](PF_6)_2$	2.038(7)	1.984(8)	1.340(12)	1.296(12)	1.431(13)	[85]
$[Ru(trpy)(3,5\text{-}^tBu_2C_6H_2O_2)(OH_2)](ClO_4)_2$	1.968(3)	2.028(3)	1.293(5)	1.280(5)	1.466(6)	[106]
$[Ru(trpy)(C_6H_4ONH)Cl]ClO_4$	1.942(8)	2.053(6)	1.270(11)	1.312(12)	1.433(13)	[35]
$[Ru(trpy)(4\text{-}^tBuC_6H_3ONH)(Cl)](ClO_4)$[b]	2.072(11)	1.975(11)	1.310(17)	1.341(19)	1.420(2)	[100]
$[Ru(trpy)(4,6\text{-}^tBu_2C_6H_2ONPh)(NO)](PF_6)_2$	1.965(2)	2.078(3)	1.324(4)	1.349(4)	1.441(5)	[118]
$[Ru(trpy)(4,6\text{-}^tBu_2C_6H_2ONPh)(OAc)](PF_6)$	2.015(6)	1.985(8)	1.281(10)	1.346(11)	1.468(13)	[100]
$[Ru(trpy)(C_6H_4NHNH)Cl]ClO_4$	1.985(6)	1.991(7)	1.317(9)	1.316(9)	1.419(11)	[35]
$Ru(bbp)(C_6H_4NHNH)(NCMe)$	1.980(5)	1.967(5)	1.328(8)	1.326(7)	1.450(8)	[119]
$Ru(bbp)(C_6H_4NHNH)(NH_2CH_2Me)$	1.993(4)	1.997(4)	1.330(6)	1.341(6)	1.438(7)	[119]
Class C						
$Ru(3,5\text{-}^tBu_2C_6H_2O_2)(PPh_3)_2(CO)Cl$	2.026(3)	2.145(3)	1.291(6)	1.296(6)	1.460(7)	[73]
$[Ru(3,5\text{-}^tBu_2C_6H_2O_2)(bpy)_2]ClO_4$	2.030(8)	2.050(8)	1.289(14)	1.327(15)	1.445(18)	[120]
$Ru(trpy)(3,5\text{-}^tBu_2C_6H_2O_2)(OAc)$	2.030(3)	2.019(3)	1.328(4)	1.324(4)	1.430(5)	[106]
$[Ru(trpy)(3,5\text{-}^tBu_2C_6H_2O_2)(DMSO)]PF_6$	2.075(4)	2.039(3)	1.320(6)	1.315(6)	1.451(7)	[121]
$Ru(trpy)(3,5\text{-}^tBu_2C_6H_2O_2)Cl$[b]	2.01(1)	2.03(1)	1.33(1)	1.30(2)	1.41(3)	[97]
$Ru(trpy)(C_6H_4O_2)(OAc)$	2.011(4)	2.064(4)	1.333(6)	1.334(6)	1.406[c]	[97]
$[Ru(trpy)(3,6\text{-}^tBu_2C_6H_2O_2)(CO)]BF_4$	2.052(5)	2.062(5)	1.301(8)	1.283(9)	1.43(1)	[122]
$[Ru(trpy)(3,5\text{-}^tBu_2C_6H_2O_2)(CO)]ClO_4$	2.075(3)	2.057(3)	1.299(4)	1.293(4)	1.451(5)	[102]
$[Ru(trpy)(4\text{-}ClC_6H_3O_2)(PPh_3)](ClO_4)$	2.082(4)	2.092(4)	1.289(7)	1.304(7)	1.432(9)	[96]
Class D						
$Ru(C_6H_4O_2)(PPh_3)_2(CO)_2$[a]	2.061(2)		1.347(4)		1.403(7)	[79]
$(NEt_4)[Ru(Cl_4C_6O_2)(CN)(CO)_2(PPh_3)]$	2.088(2)	2.077(2)	1.330(4)	1.314(4)	1.434(4)	[77]
$Ru(C_6H_4O_2)(PMe_3)_4$	2.112(4)	2.130(4)	1.352(7)	1.329(7)	1.427(8)	[80]
$Ru(trpy)(4\text{-}ClC_6H_3O_2)(PPh_3)$	2.102(5)	2.120(6)	1.320(10)	1.343(9)	1.44(1)	[96]
$Ru(C_6H_4NHNH)(PPh_3)_3$	2.05(1)	2.01(1)	1.39(2)	1.38(2)	1.43(2)	[78]

For iminoquinone/iminosemiquione/amidophenolate systems E_1 = O and E_2 = N.
[a] Ligand lies on crystallographic twofold axis.
[b] Values for one isomer.
[c] The standard deviation of this distance was not reported in the CIF available at Cambridge Structural Database.

bidentate NIL in the equatorial plane with the phosphine ligands occupying the remaining apical positions. The lability of the chloride ligands in $Ru(NIL)(PPh_3)_2Cl_2$ is established, and this motif holds the potential to be a versatile precursor to more catalytically interesting complexes [83]. The diamagnetic $Ru(3,5\text{-}^tBu_2C_6H_2O_2)(PPh_3)_2Cl_2$ compound is described by the authors as a spin-coupled Ru^{III}–NIL$^\bullet$ species [83]. The compound displays C–O distances (1.298(6) and 1.305(6) Å) and C_1–C_2 distances (1.432(6) Å) which suggest a semiquinone oxidation state. The electronic spectrum of $Ru(3,5\text{-}^tBu_2C_6H_2O_2)(PPh_3)_2Cl_2$ displays a weak absorption band at 509 nm and a more intense band at 700 nm, the low-energy band often being associated with complexes containing NIL$^\bullet$ (Table 4). The related compound $Ru(C_6H_4ONH)(PPh_3)_2Cl_2$ is also assigned as Ru^{III}–NIL$^\bullet$ based on crystallographic studies [56]. The C_6H_4ONH ligand is bisected by a twofold axis, forcing the unsymmetrical ligand to display an averaged C–O and C–N distance. The distance of 1.308(4) Å corresponds to a NIL$^\bullet$ state for C–O and a NIL^{Ox} for C–N. The elec-

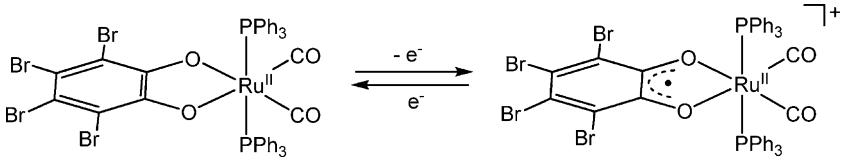

Scheme 4.

Table 3
EPR data of paramagnetic Ru–NIL complexes.

Complex	g[a]	Temperature (K)	Solvent	Ref.
$[Ru^{III}(bpy)_3]^{3+}$	2.64, 1.14	77		[123]
$[Ru^{III}(acac)_3]$	2.45, 2.16, 1.45	77		[124]
$[Cl_4C_6O_2]^-$	2.00527			[125]
$[3,5\text{-}^tBu_2C_6H_2O_2]^-$	2.0047	320	THF	[126]
Class A				
$[Ru(C_6H_4ONH)(acac)_2]^+$	2.2278, 2.1468, 1.9232	110	MeCN	[34]
$[Ru(C_6H_4NHNH)(NH_3)_4]^{3+}$	2.69, 2.42, 1.72	77	CH_3CN:toluene (2:3)	[36]
$[Ru(4,5\text{-}(OMe)_2C_6H_2NHNH)(NH_3)_4]^{3+}$	2.63–2.53,[b] 1.67	77	CH_3CN:toluene (2:3)	[36]
$[Ru(4,5\text{-}Cl_2C_6H_2NHNH)(NH_3)_4]^{3+}$	2.71, 2.39, 1.73	77	CH_3CN:toluene (2:3)	[36]
$[Ru(trpy)(3,5\text{-}^tBu_2C_6H_2ONH)Cl]^{2+}$	2.011	77	MeCN	[35]
$[Ru(trpy)(3,5\text{-}^tBu_2C_6H_2NHNH)Cl]^{2+}$	2.014	77	MeCN	[35]
Class B				
$Ru(NPh\text{–}bpa)(3,5\text{-}^tBu_2C_6H_2O_2)$	2.060, 2.025	5	CH_2Cl_2	[103]
Class C				
$[Ru(Cl_4C_6O_2)(CO)_2(PPh_3)_2]^+$	2.004	298	CH_2Cl_2	[68]
$[Ru(Br_4C_6O_2)(CO)_2(PPh_3)_2]^+$	2.007	298	CH_2Cl_2	[68]
	2.00, 2.02	77	CH_2Cl_2	[68]
$Ru(3,5\text{-}^tBu_2C_6H_2O_2)(PPh_3)_2(CO)Cl$	2.003	298	CH_2Cl_2	[73]
$Ru(Cl_4C_6O_2)(PPh_3)_2(CO)Cl$	2.002	298	CH_2Cl_2	[73]
$Ru(Cl_4C_6O_2)(PPh_3)_2(CO)H$	2.006	298	CH_2Cl_2	[73]
$Ru(Cl_4C_6O_2)(CN)(CO)_2(PPh_3)$	2.0018	294	CH_2Cl_2	[77]
$Ru(Cl_4C_6O_2)(CN)(CO)_2(P(OPh)_3)$	2.0030	294	CH_2Cl_2	[77]
$[Ru(Cl_4C_6O_2)(NCMe)(CO)_2(PPh_3)]^+$	2.0029	294	CH_2Cl_2	[77]
$[Ru(C_6H_4O_2)(bpy)_2]^+$	2.000	100	CH_2ClCH_2Cl	[66]
$[Ru(3,5\text{-}^tBu_2C_6H_2O_2)(bpy)_2]^+$	2.003	298	CH_2ClCH_2Cl	[86]
	1.985, 2.067	77	DMF	[86]
$Ru(4\text{-}(CH_2CO_2)C_6H_3O_2)(NH_3)_4$	2.722, 1.889	196	H_2O:glycerol (1:1)	[42]
$[Ru(C_6H_4O_2)(NH_3)_4]^+$	2.30	78	CH_3OH/H_2O	[90]
$[Ru(4\text{-}CO_2HC_6H_3O_2)(NH_3)_4]^+$	2.08	78	$HCl/CH_3OH/H_2O$	[90]
$[Ru(4\text{-}CO_2HC_6H_3O_2)(NH_3)_4]^+$	2.30	78	CH_3OH/H_2O	[90]
$[Ru(C_6H_4ONH)(bpy)_2]^+$	2.000	100	CH_2ClCH_2Cl	[66]
$[Ru(C_6H_4ONH)(acac)_2]^-$	2.0922, 2.0922, 1.8870	110	MeCN	[34]
$[Ru(4,6\text{-}^tBu_2C_6H_2ONPh)(bpy)_2]^+$	2.0049	298	CH_2Cl_2	[38]
	2.0393, 2.0022, 1.9728	5	CH_2Cl_2	[38]
$[Ru(C_6H_4NHNH)(bpy)_2]^+$	1.997	100	2-Me-THF	[66]
$[Ru(trpy)(4\text{-}ClC_6H_3O_2)(PPh_3)]^+$	2.00	RT	CH_2Cl_2	[96]
$[Ru(trpy)(3,5\text{-}^tBu_2C_6H_2O_2)(NH_3)]^+$	2.008	RT	CH_2Cl_2	[101]
$[Ru(trpy)(3,6\text{-}^tBu_2C_6H_2O_2)(CO)]^+$	2.00	4	CH_2Cl_2	[122]
$[Ru(trpy)(3,5\text{-}^tBu_2C_6H_2O_2)(CO)]^+$	2.00	300	CH_2Cl_2	[102]
$Ru(trpy)(3,5\text{-}^tBu_2C_6H_2O_2)(OAc)$	2.104, 2.042, 1.951	20	CH_2Cl_2/MeOH (95:5)	[41]
$Ru(trpy)(4\text{-}^tBuC_6H_3O_2)(OAc)$	2.175, 2.086, 1.910	20	CH_2Cl_2/MeOH (95:5)	[41]
$Ru(trpy)(4\text{-}ClC_6H_3O_2)(OAc)$	2.229, 2.116, 1.871	20	CH_2Cl_2/MeOH (95:5)	[41]
$Ru(trpy)(3,5\text{-}Cl_2C_6H_2O_2)(OAc)$	2.226, 2.121, 1.862	20	CH_2Cl_2/MeOH (95:5)	[41]
$Ru(trpy)(Cl_4C_6O_2)(OAc)$	2.242, 2.097, 1.846	20	CH_2Cl_2/MeOH (95:5)	[41]
$Ru(trpy)(3,5\text{-}^tBu_2C_6H_2O_2)(Cl)$	2.0	298	CH_2Cl_2:toluene (1:1)	[98]
$[Ru(trpy)(3,5\text{-}^tBu_2C_6H_2O_2)(DMSO)]^+$	2.00	293	CH_2Cl_2	[123]
$Ru(trpy)(3,5\text{-}^tBu_2C_6H_2ONH)Cl$	2.0023	77	MeCN	[35]
$Ru(trpy)(3,5\text{-}^tBu_2C_6H_2NHNH)Cl$	2.0051	77	MeCN	[35]
$[Ru(NH_2\text{–}L)(3,5\text{-}^tBu_2C_6H_2O_2)]^+$	2.015	193	CH_2Cl_2	[104]
$[Ru(NPh\text{–}bpa)(3,5\text{-}^tBu_2C_6H_2O_2)]^-$	2.175, 2.105, 1.950	20	DME	[103]

[a] Anisotropic values are listed in the order g_1 g_2 g_3 or $g_\perp$ $g_{||}$.
[b] A range for g_1 and g_2 values was reported.

tronic spectrum of $Ru(C_6H_4ONH)(PPh_3)_2Cl_2$ displays a maximum absorption band at 556 nm [56] indicative of a Ru^{II}–NIL^{Ox} species. Our preliminary DFT calculations predict a Ru^{II}–NIL^{Ox} ground state in CH_2Cl_2 solution with the triplet Ru^{III}–$NIL^{\bullet}$ electronic state 1.5 kcal/mol higher in energy. Our calculations suggest participation of both the Ru^{II}–NIL^{Ox} and Ru^{III}–$NIL^{\bullet}$ singlet resonance structures in the ground state of $Ru(C_6H_4ONH)(PPh_3)_2Cl_2$ [75]. The $Ru(NIL)(PPh_3)_2Cl_2$ systems highlight the difficulty in assigning oxidation states for Class B compounds and the risk of assigning oxidation states based on one characterization technique. Other inconsistent assignments of Class B complexes appear in the literature; $Ru(C_6H_4ONH)(acac)_2$ is one recently addressed. The complex was initially assigned as the Ru^{III}–$NIL^{\bullet}$ species based on crystallographic studies, but subsequent DFT calculations indicate contributions from both the Ru^{III}–$NIL^{\bullet}$ and Ru^{II}–NIL^{Ox} resonance forms [34,40]. Interestingly, the UV–vis spectra of this $Ru(C_6H_4ONH)(acac)_2$ and the one-electron-reduced Class C species show λ_{max} at 531 and 715 nm [34] suggesting Ru^{II}–NIL^{Ox} and Ru^{II}–$NIL^{\bullet}$ assignments, respectively.

4.4. L and L′ = polypyridyl or amine

Heteroleptic ruthenium polypyridyl complexes containing NILs have been investigated extensively for over 20 years. As these systems have been the subject of a number of review articles in the past, their discussion here will be limited [25,29,30,33,44,55,62,63]. The first report of a ruthenium polypyridyl NIL complex was that of Belser et al. [85]. A series of benzoquinonediimine complexes were synthesized and the crystal structure of the Class B complex $[Ru(C_6H_4NHNH)(bpy)_2]^{2+}$ was determined, displaying intermediate C–N distances of 1.296 and 1.340 Å indicative of an electronic configuration somewhere between that of Ru^{II}–NIL^{Ox}

Table 4
Electronic Spectra for Ru–NIL complexes[a].

Complex	Wavelength in nm (ε, M^{-1} cm^{-1})	Solvent	Ref.
Class A			
$[Ru(C_6H_4ONH)(acac)_2]^+$	400, 590 (6500)	MeCN	[34]
$[Ru(trpy)(C_6H_4ONH)Cl]^{2+}$	232 (29400), 308 (19600), 324 (17400), 438 (4500), 475 (3900)	MeCN	[35]
$[Ru(4,6\text{-}^tBu_2C_6H_2ONPh)(bpy)_2]^{3+}$	309 (26100), 437 (8100), 504 (8100), 591 (sh)	CH_2Cl_2	[38]
$[Ru(C_6H_4NHNH)(NH_3)_4]^{3+}$	220, 324, 416 (15136), 497 (1479), 800	0.1 M H_3PO_4	[36]
$[Ru(4,5\text{-}(OMe)_2C_6H_2NHNH)(NH_3)_4]^{3+}$	232, 322, 426 (14125), 524 (776)	0.1 M H_3PO_4	[36]
$[Ru(4,5\text{-}Cl_2C_6H_2NHNH)(NH_3)_4]^{3+}$	240, 338, 424 (14125), 510 (1318)	0.1 M H_3PO_4	[36]
$[Ru(C_6H_4NHNH)(edta)]^-$	330 (< 3000), 458 (12000), 575 (sh)	0.1 M aq. CF_3CO_2Na	[37]
$[Ru(trpy)(C_6H_4NHNH)Cl]^{2+}$	232 (26300), 270 (17750), 282 (16330), 308 (15580), 327 (12070), 440 (5030), 487 (6630)	MeCN	[35]
Class B			
$Ru(3,5\text{-}^tBu_2C_6H_2O_2)(PPh_3)_2Cl_2$	509, 700	CH_2Cl_2	[83]
$[Ru(C_6H_4O_2)(bpy)_2]^{2+}$	299 (sh), 360 (7586), 391 (7586), 641 (13183)	CH_2ClCH_2Cl	[66]
$[Ru(3,5\text{-}^tBu_2C_6H_2O_2)(bpy)_2]^{2+}$	372 (7586), 400 (sh,7244), 669 (14125)	CH_2ClCH_2Cl	[86]
$[Ru(Cl_4C_6O_2)(bpy)_2]^{2+}$	381 (5370), 639 (11220)	CH_2ClCH_2Cl	[86]
$[Ru(C_6H_4O_2)(py)_4]^{2+}$	333 (11482), 641 (5754)	CH_2ClCH_2Cl	[66]
$[Ru(4\text{-}^tBuC_6H_3O_2)(py)_4]^{2+}$	360 (sh,4571), 380 (sh,3090), 673 (10471)	CH_2ClCH_2Cl	[86]
$[Ru(Cl_4C_6O_2)(py)_4]^{2+}$	404 (br,3311), 623 (11482)	CH_2ClCH_2Cl	[86]
$[Ru(C_6H_4O_2)(NH_3)_4]^{2+}$	272 (6700), 360 (sh), 450 (sh), 515 (7600)	H_2O (pH 7)	[90]
$[Ru(4\text{-}OMeC_6H_3O_2)(NH_3)_4]^{2+}$	270, 360 (sh), 441 (sh), 510 (8500)	H_2O (pH 7)	[90]
$[Ru(4\text{-}CO_2C_6H_3O_2)(NH_3)_4]^+$	284, 360 (sh), 457 (sh), 519 (7600)	H_2O (pH 7)	[90]
$[Ru(4\text{-}CO_2C_6H_3O_2)(NH_3)_4]^+$	286, 460, 520	H_2O (pH 7)	[91]
$[Ru(C_6H_4O_2)(edta)]^{2-}$	263 (8000), 346 (1600), 532 (9100)	H_2O (pH 10)	[127]
$[Ru(3,5\text{-}(SO_3)_2C_6H_2O_2)(edta)]^{4-}$	280 (7050), 295 (2100), 540 (6100)	H_2O (pH 10)	[127]
$[Ru(4\text{-}CO_2C_6H_3O_2)(edta)]^{3-}$	245 (7500), 270 (7500), 540 (7200)	H_2O (pH 10)	[127]
$[Ru(C_6H_4ONH)(bpy)_2]^{2+}$	366 (8511), 435, 488 (7586), 575 (12589)	CH_2ClCH_2Cl	[66]
$[Ru(4,6\text{-}^tBu_2C_6H_2ONPh)(bpy)_2]^{2+}$	281 (31100), 411 (5800), 595 (13400)	CH_2Cl_2	[38]
$Ru(C_6H_4ONH)(PPh_3)_2Cl_2$	232 (86500), 288 (54500), 348 (8000), 466 (5700), 556 (5900)	CH_2Cl_2	[56]
$Ru(C_6H_4ONH)(acac)_2$	350, 420, 531 (8050)	MeCN	[34]
$[Ru(C_6H_4NHNH)(Me_3tacn)I]^+$	260 (11400), 393 (38000), 530 (9100), 891 (80)	MeCN	[116]
$[Ru(C_6H_4NHNH)(Me_3tacn)(N_3)]^+$	260 (8800), 357 (1900), 516 (10000), 889 (80)	MeCN	[116]
$[Ru(C_6H_4NHNH)(Me_3tacn)(OH_2)]^{2+}$	256 (14600), 504 (16 000), 888 (100)	H_2O	[116]
$[Ru(C_6H_4NHNH)(Me_3tacn)(NCMe)]^{2+}$	245 (22000), 509 (15000), 830 (180)	MeCN	[116]
$[Ru(C_6H_4NHNH)(bpy)_2]^{2+}$	242 (4571), 281 (40738), 324 (sh), 445 (sh, 7762), 515 (21878), 755 (661)	CH_3CN	[65,66]
$[Ru(4,5\text{-}OMe)_2C_6H_2NHNH](bpy)_2]^{2+}$	285, 436 (7079), 531 (30903), 667 (251)	CH_3CN	[65]
$[Ru(C_6H_4NHNH)(edta)]^{2-}$	255 (< 10000), 480 (12000)	0.1 M aq. CF_3CO_2Na	[37]
$[Ru(4,5\text{-}Me_2C_6H_2NHNH)(bpy)_2]^{2+}$	282, 450 (7943), 521 (25119), 730 (214)	CH_3CN	[65]
$[Ru(4,5\text{-}Me_2C_6H_2NHNH)(bpy)_2]^{2+}$	351 (8511), 444 (sh), 457 (8511), 504 (10471), 524 (sh), 620 (10471)	CH_3CN	[65]
$[Ru(4,5\text{-}(NH_2)_2C_6H_2NHNH)(bpy)_2]^{2+}$	289, 474 (10965), 552 (37153), 641 (sh)	CH_3CN	[65]
$[Ru(4,5\text{-}(NH_3)_2C_6H_2NHNH)(bpy)_2]^{4+}$	390 (5370), 508 (20893), 905 (229)	*Conc.* H_2SO_4	[65]
$[Ru(4,5\text{-}(NH_3)(NH_2)C_6H_2NHNH)(bpy)_2]^{3+}$	442 (7079), 532 (26915), 727 (457)	3 M HCl	[65]
$[Ru(4,5\text{-}Cl_2C_6H_2NHNH)(bpy)_2]^{2+}$	280 (41687), 421 (5623), 525 (25119), 791 (117)	CH_3CN	[65]
$[Ru(4\text{-}NO_2C_6H_3NHNH)(bpy)_2]^{2+}$	279 (37154), 416 (7943), 527 (20417), 851 (309)	CH_3CN	[65]
$[Ru(C_6H_4NHNH)(py)_4]^{2+}$	239 (27542), 289 (sh,10715), 313 (11749), 535 (13804)	CH_2ClCH_2Cl	[66]
$[Ru(C_6H_4NHNH)(NH_3)_4]^{2+}$	196, 258 (9772), 470 (10233), 965	0.1 M H_3PO_4	[36]
$[Ru(4,5\text{-}(OMe)_2C_6H_2NHNH)(NH_3)_4]^{2+}$	200, 260 (10715), 498 (10000), 893	0.1 M H_3PO_4	[36]
$[Ru(4,5\text{-}Cl_2C_6H_2NHNH)(NH_3)_4]^{2+}$	210, 274 (9772), 478 (11220), 1031	0.1 M H_3PO_4	[36]
$Ru(C_6H_4NHNH)(NH_3)_2Cl_2$	262 (8100), 317sh, 500 (10000), 917 (52), 1020 sh	H_2O	[113]
$Ru(C_6H_4NHNPh)(bpy)Cl_2$	240 (16950), 290 (19560), 540 (11690), 830 (140), 1065 (90)	MeCN	[128]
$Ru(C_6H_4NHNPh)(NH_2Ph)_2Cl_2$	365 (2650), 492 (6840), 585 (2070)	CH_2Cl_2	[71]
$Ru(C_6H_4NHNH)(acac)_2$	265 (16980), 300 (7080), 500 (6760), 950 (60)	MeCN	[114]
$Ru(C_6H_4NHNPh)(acac)_2$	275 (24550), 320 (10720), 519 (19050), 1025 (90)	MeCN	[114]
$[Ru(trpy)(3,5\text{-}^tBu_2C_6H_2O_2)(NH_3)]^{2+}$	615 (13000)	CH_2Cl_2	[101]
$[Ru(trpy)(C_6H_4O_2)(OAc)]^+$	212 (20000) 324 (14800), 556 (14100)	Acetone	[97]
$[Ru(trpy)(3,5\text{-}^tBu_2C_6H_2O_2)(OAc)]^+$	214 (22000), 326 (15800), 584 (16900)	Acetone	[97]
$[Ru(trpy)(3,5\text{-}^tBu_2C_6H_2O_2)Cl]^+$	212 (20000) 328 (14500), 592 (15500)	Acetone	[97]
$[Ru(trpy)(3,5\text{-}^tBu_2C_6H_2O_2)(OH_2)]^{2+}$	600 (16800)	CH_2Cl_2	[106,129]
$[Ru(trpy)(3,5\text{-}^tBu_2C_6H_2O_2)(OH)]^+$	576 (16700)	CH_2Cl_2	[129]
$[Ru(trpy)(4\text{-}ClC_6H_3O_2)(OH_2)]^{2+}$	567 (5600)	CH_2Cl_2	[106]
$[Ru(trpy)(C_6H_4ONH)Cl]^+$	232 (35280), 270 (24910), 311 (24630), 459 (8200), 483 (10400), 556 (19790)	MeCN	[35]
$[Ru(trpy)(C_6H_4ONH)Cl]^+$	552 (15600)	Acetone	[100]
$[Ru(trpy)(4\text{-}^tBuC_6H_3ONH)Cl]^+$	567 (15500)	Acetone	[100]
$[Ru(trpy)(4\text{-}^tBuC_6H_3ONH)(OAc)]^+$	565 (16900)	Acetone	[100]
$[Ru(trpy)(5\text{-}MeC_6H_3ONH)(OAc)]^+$	557 (17600)	Acetone	[100]
$[Ru(trpy)(4\text{-}MeC_6H_3ONH)(OAc)]^+$	566 (16100)	Acetone	[100]
$[Ru(trpy)(C_6H_4ONH)(OAc)]^+$	553 (17000)	Acetone	[100]
$[Ru(trpy)(5\text{-}ClC_6H_3ONH)(OAc)]^+$	553 (18300)	Acetone	[100]
$[Ru(trpy)(4\text{-}ClC_6H_3ONH)(OAc)]^+$	559 (15100)	Acetone	[100]
$[Ru(trpy)(4,6\text{-}^tBu_2C_6H_2ONPh)(OAc)]^+$	568 (19200)	Acetone	[100]
$[Ru(trpy)(4,6\text{-}^tBu_2C_6H_3ON(2\text{-}CF_3Ph)(OAc)]^+$	562 (17300)	Acetone	[100]
$[Ru(trpy)(4,6\text{-}^tBu_2C_6H_2ONPh)Cl]^+$	237 (44246), 270 (34080), 315 (29940), 570 (24092)	CH_2Cl_2	[118]
$[Ru(trpy)(C_6H_4NHNH)Cl]^+$	232 (28000), 274 (21000), 280 sh (20000), 316 (22000), 506 (16000)	H_2O	[99]
$[Ru(trpy)(C_6H_4NHNH)Cl]^+$	208 (28930), 234 (22690), 269 (18330), 280 (16190), 311 (17210), 509 (15670)	MeCN	[35]
$[Ru(trpy)(C_6H_4NHNH)(OH_2)]^{2+}$	234 (29000), 272 (22000), 280 (22000), 314 (21000), 496 (24000)	H_2O	[99]
$Ru(bbp)(C_6H_4NHNH)(NCMe)$	339 (9548), 518 (4816)	MeCN	[119]

Table 4 (*Continued*)

Complex	Wavelength in nm (ε, M^{-1} cm^{-1})	Solvent	Ref.
Ru(bbp)(C_6H_4NHNH)(NH_2CH_2Me)	248 (39429), 319 (12960), 508 (3988)	MeCN	[119]
[Ru(NH_2–L)(3,5-$^tBu_2C_6H_2O_2$)]$^{2+}$	618 (7890)	CH_2Cl_2	[104]
Ru(NPh–bpa)(3,5-$^tBu_2C_6H_2O_2$)	366 (6620), 638 (5210), 906 (5060)	CH_2Cl_2	[103]
[Ru(NHPh-bpa)(3,5-$^tBu_2C_6H_2O_2$)]$^+$	370 (4980), 558 (5070), 872 (9450), 1172 (4470)	CH_2Cl_2	[103]
[Ru_2(btpyxa)(3,6-$^tBu_2C_6H_2O_2$)$_2$(Cl_2)]$^{2+}$	598 (19300)	CH_2Cl_2	[130]
[Ru_2(btpyan)(3,6-$^tBu_2C_6H_2O_2$)$_2$(OH_2)]$^{2+}$	576 (5700)	MeOH	[23]
Ru_2(btpyan)(3,6-$^tBu_2C_6H_2O_2$)$_2$(O_2)	850	MeOH	[23]
Class C			
[Ru($Cl_4C_6O_2$)(PPh_3)$_2$(CO_2]$^+$	368 sh (3200), 425 (3400), 480 (3200), 580 sh (2300)	CH_2Cl_2	[68]
[Ru($Br_4C_6O_2$)(PPh_3)$_2$(CO_2]$^+$	335 sh (5700), 385 (4300), 415 (4200), 518 (4500), 595 (4100)	CH_2Cl_2	[68]
Ru($Cl_4C_6O_2$)(PPh_3)$_2$(CO)H	230 (49020), 272 (23455), 336 (4190), 368 (3830), 496 (sh) (1135), 610 (2180), 754 (2790), 1060 (1260)	CH_2Cl_2	[73]
Ru($Cl_4C_6O_2$)(PPh_3)$_2$(CO)Cl	230 (45 030), 370 (3630), 502 (sh) (1240), 608 (2150), 674 (2120), 744 (2425), 934 (940), 1058 (940)	CH_2Cl_2	[73]
Ru(3,5-$^tBu_2C_6H_2O_2$)(PPh_3)$_2$(CO)Cl	238 (28890), 256 (23590), 502 (1985), 642 (2390), 878 (820), 1002 (615)	CH_2Cl_2	[73]
[Ru($C_6H_4O_2$)(bpy)$_2$]$^+$	344 (8913), 493 (2512), 515 (sh), 580 (sh), 889 (13490)	CH_2ClCH_2Cl	[86]
[Ru($Cl_4C_6O_2$)(bpy)$_2$]$^+$	336 (sh), 450 (br,5495), 519 (sh), 939 (15849)	CH_2ClCH_2Cl	[86]
[Ru(3,5-$^tBu_2C_6H_2O_2$)(bpy)$_2$]$^+$	348 (13490), 494 (9120), 525 (sh), 601 (sh), 844 (15488), 1198 (741)	CH_2ClCH_2Cl	[86]
[Ru($C_6H_4O_2$)(py)$_4$]$^+$	244 (13490), 358 (13183), 556, 943 (8913)	CH_2ClCH_2Cl	[66]
[Ru(4-$^tBuC_6H_3O_2$)(py)$_4$]$^+$	320 (sh,7762), 374 (14125), 926 (11481), 1149 (sh,741)	CH_2ClCH_2Cl	[86]
[Ru($Cl_4C_6O_2$)(py)$_4$]$^+$	327 (16982), 976 (10715)	CH_2ClCH_2Cl	[86]
Ru(4-$CO_2C_6H_3O_2$)(NH_3)$_4$	213 (24100), 266 (9300), 295 (8200), 665 (2800)	H_2O (pH 7)	[91,95]
[Ru(4-$C_2H_4NH_2C_6H_3O_2$)(NH_3)$_4$]$^+$	280 (3162), 319 (676), 429 (398), 680 (1047)	H_2O (pH 7)	[91]
[Ru(4-CH(OH)$CH_2NH_2C_6H_3O_2$)(NH_3)$_4$]$^+$	290 (3548), 360 (2630), 672 (1995)	H_2O (pH 7)	[91]
[Ru(4-CH(OH)$CH_2NHCH(CH_3)_2C_6H_3O_2$)($NH_3$)$_4$]$^+$	289 (4266), 330 (2089), 423 (631), 666 (2188)	H_2O (pH 7)	[91]
[Ru(4-$OMeC_6H_3O_2$)(NH_3)$_4$]$^+$	212 (18200), 278 (sh), 690 (2900)	H_2O (pH 7)	[90]
[Ru($C_6H_4O_2$)(edta)]$^{3-}$	244 (6400), 284 (5100), 420 (650), 680 (2100)	H_2O (pH 10)	[127]
[Ru(4-$C_2H_4NH_2C_6H_3O_2$)(edta)]$^{3-}$	416 (550), 684 (2300)	H_2O (pH 10)	[94]
[Ru(4-$CO_2C_6H_3O_2$)(edta)]$^{4-}$	240 (9600), 300 (6400), 400 (860), 668 (2100)	H_2O (pH 10)	[127]
[Ru(3,5-$(SO_3)_2C_6H_2O_2$)(edta)]$^{5-}$	245 (7200), 310 (5300), 388 (1500), 640 (2200)	H_2O (pH 10)	[127]
[Ru(4-$C_2H_4(CO_2H)NH_2C_6H_3O_2$)(edta)]$^{4-}$	420 (600), 684 (2000)	H_2O (pH 10)	[94]
[Ru(C_6H_4ONH)(bpy)$_2$]$^+$	350 (10000), 382 (9772), 495 (8511), 524 (8913), 680 (10000), 820 (sh,1259)	CH_2ClCH_2Cl	[66]
[Ru(4,6-$^tBu_2C_6H_2ONPh$)(bpy)$_2$]$^+$	294 (36000), 350 (9500), 376 (sh), 496 (6300), 686 (7400)	CH_2Cl_2	[38]
[Ru(C_6H_4ONH)(acac)$_2$]$^-$	375 (7220), 415 (6670), 715 (5350),	MeCN	[34]
[Ru(C_6H_4NHNH)(bpy)$_2$]$^+$	349 (8128), 435 (7586), 454 (sh), 496 (9120), 535 (sh), 625 (11220), 939 (1047)	CH_3CN	[65,66]
[Ru(4,5-$(OMe)_2C_6H_2NHNH$)(bpy)$_2$]$^+$	338, 357 (sh), 455, 476, 513, 524 (sh), 615	CH_3CN	[65]
[Ru(4,5-$Cl_2C_6H_2NHNH$)(bpy)$_2$]$^+$	321 (sh), 476 (11749), 651 (14454), 813	CH_3CN	[65]
[Ru(4-$NO_2C_6H_3NHNH$)(bpy)$_2$]$^+$	303 (sh), 413 (sh), 455 (11749), 649 (17378), 808	CH_3CN	[65]
[Ru(C_6H_4NHNH)(py)$_4$]$^+$	393 (14454), 535, 660 (10471)	CH_2ClCH_2Cl	[66]
[Ru(trpy)(4-$ClC_6H_3O_2$)(PPh_3)]$^+$	274 (21700), 313 (25900), 479 (4270), 832 (10000)	CH_2Cl_2	[96]
[Ru(trpy)(3,5-$^tBu_2C_6H_2O_2$)(NH_3)]$^+$	854 (13000)	CH_2Cl_2	[101]
[Ru(trpy)(3,6-$^tBu_2C_6H_2O_2$)(CO)]$^+$	388, 625	CH_2Cl_2	[122]
[Ru(trpy)(3,5-$^tBu_2C_6H_2O_2$)(CO)]$^+$	284 (2540), 310 (2250), 274 (2330), 324 (2580), 396 (3430), 644 (4390)	CH_2Cl_2	[102]
Ru(trpy)(3,5-$^tBu_2C_6H_2O_2$)(OAc)	214 (40700), 317 (24000), 370 (5400), 576 (3300), 883 (18600)	CH_2Cl_2	[41,106]
Ru(trpy)($C_6H_4O_2$)(OAc)	225 (31600), 279 (24000), 316 (22900), 371 (5400), 534 (3500), 878 (15100)	CH_2Cl_2	[97]
Ru(trpy)(4-$NO_2C_6H_3O_2$)(OAc)	225 (26900), 277 (20400), 317 (19500), 371 (7600), 506 (4400), 829 (8300), 855 (8100)	CH_2Cl_2	[97]
Ru(trpy)(4-$^tBuC_6H_3O_2$)(OAc)	897 (15300)	CH_2Cl_2	[41]
Ru(trpy)(4-$ClC_6H_3O_2$)(OAc)	890 (15200)	CH_2Cl_2	[41]
Ru(trpy)(3,5-$Cl_2C_6H_2O_2$)(OAc)	885 (14100)	CH_2Cl_2	[41]
Ru(trpy)($Cl_4C_6O_2$)(OAc)	226 (50100), 277 (25700), 315 (24500), 511 (3200), 849 (11500), 884 (11700)	CH_2Cl_2	[41,97]
Ru(trpy)(3,5-$^tBu_2C_6H_2O_2$)Cl	240 (27200), 272 (17900), 282 (20200), 320 (20700), 372 (5300), 404 (3900), 546 (3500), 586 (3600), 875 (16900)	CH_2Cl_2	[98]
Ru(trpy)(C_6H_4ONH)Cl	235 (47020), 277 (28090), 311 (29460), 399 (7920), 537 (5980), 702 (15380)	MeCN	[35]
Ru(trpy)(C_6H_4NHNH)Cl	204 (27000), 243 (20400), 309 (9020), 328 (5930), 477 (5140), 516 (4580), 718 (2530)	MeCN	[35]
[Ru(NH_2–L)(3,5-$^tBu_2C_6H_2O_2$)]$^+$	888	CH_2Cl_2	[104]
[Ru(NPh–bpa)(3,5-$^tBu_2C_6H_2O_2$)]$^-$	324 (11100), 432 (8470), 560 (7140), 886 (6540)	DME	[103]
Class D			
Ru($C_6H_4O_2$)(PPh_3)$_2$(CO_2	482 (2000)	CH_2Cl_2	[79]
Ru($Cl_4C_6O_2$)(PPh_3)$_2$(CO_2	340 sh (4000), 440 (2700)	CH_2Cl_2	[68]
Ru($Br_4C_6O_2$)(PPh_3)$_2$(CO_2	330 sh (4900), 440 (3100)	CH_2Cl_2	[68]
Ru($C_6H_4O_2$)(bpy)$_2$	333 (9333), 380 (9120), 406 – 480, 617 (8511), 730 (br,3981)	CH_2ClCH_2Cl	[66,86]
Ru($Cl_4C_6O_2$)(bpy)$_2$	366 (10715), 400 – 460, 592 (7586), 680 (br,3890)	CH_2ClCH_2Cl	[86]
Ru(3,5-$^tBu_2C_6H_2O_2$)(bpy)$_2$	380 (12589), 400 – 500, 639 (10000), 769 (6607)	CH_2ClCH_2Cl	[86]
Ru($C_6H_4O_2$)(py)$_4$	340 (8128), 394 (11749), 461 (14125), 521 (sh)	CH_2ClCH_2Cl	[66]
Ru(4-$^tBuC_6H_3O_2$)(py)$_4$	344 (7943), 410 (12303), 484 (13490), 580 (4677)	CH_2ClCH_2Cl	[86]
Ru($Cl_4C_6O_2$)(py)$_4$	338 (8710), 388 (15488), 446 (20893)	CH_2ClCH_2Cl	[86]
[Ru(4-$CO_2C_6H_3O_2$)(NH_3)$_4$]$^-$	265 (12800), 284 (12600)	H_2O (pH 7)	[90]
Ru(4-$CO_2HC_6H_3O_2$)(NH_3)$_4$	212 (24100), 297 (8200), 658 (2800)	H_2O (pH 7)	[90]
Ru($C_6H_4O_2$)(NH_3)$_4$	265 (6700), 326 (sh)	H_2O (pH 7)	[90]
Ru(4-$OMeC_6H_3O_2$)(NH_3)$_4$	< 250	H_2O (pH 7)	[90]
Ru(4,6-$^tBu_2C_6H_2ONPh$)(bpy)$_2$	295 (35600), 374 (9800), 423 (sh), 531 (7000), 607 (sh)	CH_2Cl_2	[38]
Ru(4,5-$Me_2C_6H_2NHNH$)(bpy)$_2$	356, 535	CH_3CN	[65]
Ru(4,5-$Cl_2C_6H_2NHNH$)(bpy)$_2$	373, 541	CH_3CN	[65]

Table 4 (*Continued*)

Complex	Wavelength in nm (ε, M^{-1} cm^{-1})	Solvent	Ref.
$Ru(4\text{-}NO_2C_6H_3NHNH)(bpy)_2$	366, 529, 715, 769	CH_3CN	[65]
$Ru(trpy)(4\text{-}ClC_6H_3O_2)(PPh_3)$	280 (22200), 314 (27100), 523 (5250)	CH_2Cl_2	[96]
$Ru(trpy)(3,6\text{-}^tBu_2C_6H_2O_2)(CO)$	453	CH_2Cl_2	[122]
$Ru(trpy)(3,5\text{-}^tBu_2C_6H_2O_2)(CO)$	438	CH_2Cl_2	[102]
$[Ru(trpy)(C_6H_4ONH)Cl]^-$	311 (29020), 436 (14650), 521 (11720), 615 (12020)	MeCN	[35]
$[Ru(trpy)(C_6H_4NHNH)Cl]^-$	262 (29940), 325 (11860), 439 (8840) 475 (7580), 523 (5740), 596 (4180)	MeCN	[35]

[a] Molar absorptivities are listed as reported, even though we believe the significant digits are overestimated.

and Ru^{III}–NIL• [85]. This species was later investigated by Masui et al. in greater detail and assigned as Ru^{II}–NIL^{Ox} where its distinctive and intense electronic transition at 515 nm (21 900 M^{-1} cm^{-1}) was reported to show very weak charge transfer behavior [66]. The origin of this intense absorption has since been assigned to a ML→ML transition[4] (*cf.*, ν_3 in Fig. 1) [25,33,55,59,62]. The Ru(dπ) orbital is strongly stabilized by efficient backbonding onto the NIL(π^*) system resulting in the LUMO orbital having appreciable metal character. As the Ru(dπ) levels are stabilized by π-backdonation to the NIL(π^*) orbitals, the degree of mixing with the filled NIL(π) levels increases. Thus the synergistic nature of both the Ru(dπ)–NIL(π^*) and Ru(dπ)–NIL(π) interactions reduces the charge transfer character of the transition via extensive delocalization of electron density over the metal–ligand framework. Two benzoquinonediimine based reductions were observed at potentials of −0.47 and −1.15 V *vs.* SCE and were assigned to formation of the Ru^{II}–NIL• (Class C) and Ru^{II}–NIL^{Red} (Class D) species, respectively (Fig. 3).

A series of ruthenium pyridyl and polypyridyl complexes with dioxolene co-ligands was reported by Haga et al. [86] where by using bulk electrolysis the complexes were studied in three different redox states, thus allowing a direct comparison of Class B, Class C and Class D systems [86]. The Ru^{II}–$NIL^{•/Red}$ redox couple displayed an anodic shift of +0.20 and +0.35 V (Table 5) on going from $Ru(Cl_4C_6O_2)(bpy)_2$ to $Ru(C_6H_4O_2)(bpy)_2$ to $Ru(3,5\text{-}^tBu_2C_6H_2O_2)(bpy)_2$. The EPR spectrum of the oxidized Class C species $[Ru(3,5\text{-}^tBu_2C_6H_2O_2)(bpy)_2]^+$ was consistent with a predominant contribution from the Ru^{II}–NIL• resonance form (Table 3). The bond distances measured by X-ray crystallography are mostly consistent with this hypothesis, however, the C–O bond lengths of 1.289(14) and 1.327(15) Å are ambiguous, suggesting contributions from both Ru^{II}–NIL• and Ru^{III}–NIL^{Red}, respectively. The $NIL^{Ox/•}$ and $NIL^{•/Red}$ reduction potentials displayed a linear dependence on the Hammett $\Sigma\sigma$ parameters. Oxidation at potentials >1.5 V *vs.* SCE for these $Ru(NIL)(bpy)_2$ systems resulted in irreversible formation of the Class A Ru^{III}–NIL^{Ox} species consistent with there being only a few reports of such complexes isolated to date [34–38].

The LUMO orbital, a mixture of Ru(dπ) and NIL(π^*), increases in energy in the order $NIL^• < NIL^{Ox}$ [87,88] a result that is consistent with the large blue shift observed for the low-energy intense transition on going from Class C to Class B systems, e.g., $[Ru(3,5\text{-}^tBu_2C_6H_2O_2)(bpy)_2]^+$ and $[Ru(3,5\text{-}^tBu_2C_6H_2O_2)(bpy)_2]^{2+}$ display absorption maxima at 889 (13 500 M^{-1} cm^{-1}) and 641 (13 200 M^{-1} cm^{-1}) respectively (Table 4) [86]. For the Class C species this transition decreases in energy as the acceptor strength of the NIL• increases with $[Ru(3,5\text{-}^tBu_2C_6H_2O_2)(bpy)_2]^+$ (844 nm; 15 500 M^{-1} cm^{-1}) > $[Ru(C_6H_4O_2)(bpy)_2]^+$ (889 nm; 13 500 M^{-1} cm^{-1}) > $[Ru(Cl_4C_6O_2)(bpy)_2]^+$ (939 nm; 15 900 M^{-1} cm^{-1}). The opposite trend, however, is observed for the Class B systems with $[Ru(3,5\text{-}^tBu_2C_6H_2O_2)(bpy)_2]^{2+}$ (669 nm; 14 100 M^{-1} cm^{-1}) < $[Ru(C_6H_4O_2)(bpy)_2]^{2+}$ (641 nm; 13 300 M^{-1} cm^{-1}) < $[Ru(Cl_4C_6O_2)(bpy)_2]^{2+}$ (639 nm; 11 200 M^{-1} cm^{-1}). This has been explained by the greater exchange integral and π-acceptor character of the NIL^{Ox} oxidation state of the ligand which stabilizes the Ru(dπ) orbitals significantly, thus increasing the transition energy and its associated reorganization energy relative to the Class C system [59,86].

In a series of $[Ru(NIL)(bpy)_2]^n$ and $[Ru(NIL)(py)_4]^n$ systems investigated by Masui et al. (NIL = C_6H_4NHNH, C_6H_4NHO, $C_6H_4O_2$; n = 0, 1+ or 2+), it was observed that the low-energy absorption blue shifts for Class B and Class C systems with the transition energy increasing in the order O·O < NH·O < NH·NH (Fig. 4) [25,66]. Although the Ru(dπ) orbitals should be destabilized with decreased backdonation onto the NIL(π^*) ligand in the order NH·NH < NH·O < O·O, the interaction of the Ru(dπ) orbitals with the filled NIL(π) orbitals increases with the number of nitrogen atoms, thus resulting in a greater net stabilization [33,66]. EPR and XPS studies indicate a predominance of the Ru^{II}–NIL• resonance form for the Class C species whereas the Class B systems to lie somewhere in between the Ru^{II}–NIL^{Ox} and Ru^{III}–NIL• resonance structures.

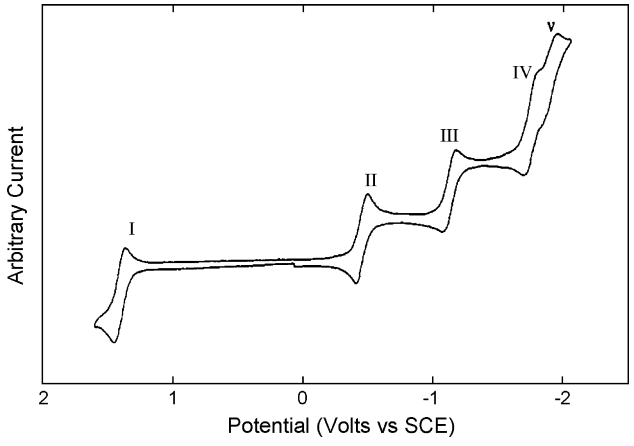

Fig. 3. Cyclic voltammogram of $[Ru(C_6H_4NHNH)(bpy)_2]^{2+}$ displaying the five independent redox couples for this species (I) $Ru^{III/II}$, (II) $NIL^{Ox/•}$, (III) $NIL^{•/Red}$, (IV) $bpy^{0/•}$, (V) $bpy^{•0/•}$. This figure was reproduced from Ref. [65] with permission of the copyright holders.

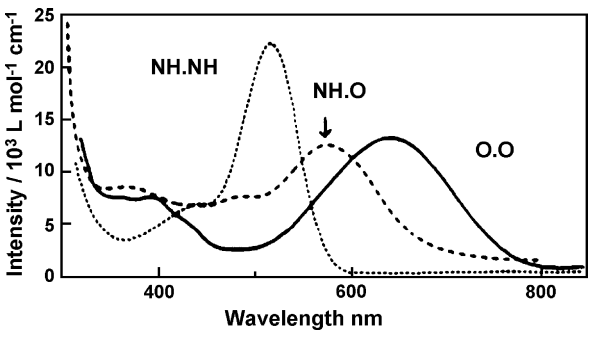

Fig. 4. The electronic spectra of Class B systems $[Ru(NIL)(bpy)_2]^{2+}$ where NIL = $C_6H_4O_2$, C_6H_4NHO, C_6H_4NHNH recorded in CH_2ClCH_2Cl (O·O and NH·O) and acetonitrile (NH·NH). This figure was reproduced from Ref. [25] with permission of the copyright holders.

Table 5
Electrochemical data for Ru–NIL complexes.

Complex	$E_{1/2}$	$E_{1/2}$	$E_{1/2}$	$E_{1/2}$	$E_{1/2}$		Solvent	Counterelectrolyte	Ref.
Class B									
$[Ru(4\text{-}CO_2C_6H_3O_2)(NH_3)_4]^+$		0.54	−0.86[b]			SCE	MeCN	H_3PO_4	[36]
$Ru(3,5\text{-}{}^tBu_2C_6H_2O_2)(PPh_3)_2Cl_2$	0.297	−0.775				Fc/Fc^+	MeCN	$TBAClO_4$	[83]
$Ru(C_6H_4ONH)(PPh_3)_2Cl_2$	0.66	−0.55[a]				SCE	CH_2Cl_2	$TBAClO_4$	[56]
$Ru(C_6H_4ONH)(acac)_2$	0.37	−0.96				SCE	MeCN	$TBAClO_4$	[34]
$Ru(C_6H_4NHNPh)(bpy)Cl_2$	0.58	−0.92	−1.3	−2.4[a]		SCE	MeCN	$TBAClO_4$	[128]
$Ru(C_6H_4NHNPh)(NH_2Ph)_2Cl_2$	0.60	−0.73[a]				SCE	MeCN	$TBAClO_4$	[71]
$Ru(C_6H_4NHNH)(NH_3)_2Cl_2$	0.47	−0.96[a]				NHE	DMF	$TBAPF_6$	[113]
$[Ru(C_6H_4NHNH)(Me_3tacn)(NCMe)]^{2+}$	0.84	−1.02	−1.80			Fc/Fc^+	MeCN	$TBAPF_6$	[116]
$[Ru(C_6H_4NHNH)(Me_3tacn)I]^+$	0.37	−1.31[a]				Fc/Fc^+	MeCN	$TBAPF_6$	[116]
$[Ru(C_6H_4NHNH)(Me_3tacn)(N_3)]^+$	0.17	−1.33	−2.31[a]			Fc/Fc^+	MeCN	$TBAPF_6$	[116]
$[Ru(C_6H_4NHNH)(bpy)_2]^{2+}$	1.35	−0.47	−1.15	−1.72[a]	−1.96[a]	SCE	MeCN	$TBAPF_6$	[66]
	1.37	−0.45	−1.13	−1.70[a]	−1.94[a]	SCE	MeCN	$TBAPF_6$	[65]
$[Ru(4,5\text{-}(OMe)_2C_6H_2NHNH)(bpy)_2]^{2+}$	1.15	−0.73	−1.26	−1.74	−1.86	SCE	MeCN	$TBAPF_6$	[65]
$[Ru(4,5\text{-}Me_2C_6H_2NHNH)(bpy)_2]^{2+}$	1.32	−0.56	−1.21	−1.71	−1.94[a]	SCE	MeCN	$TBAPF_6$	[65]
$[Ru(4\text{-}Cl_2C_6H_2NHNH)(bpy)_2]^{2+}$	1.50[a]	−0.28	−0.96	−1.75	−2.19	SCE	MeCN	$TBAPF_6$	[65]
$[Ru(4,5\text{-}(NH_2)_2C_6H_2NHNH)(bpy)_2]^{2+}$	0.83	−0.94[a]	−1.43	−1.78	−2.01	SCE	MeCN	$TBAPF_6$	[65]
$[Ru(4\text{-}NO_2C_6H_2NHNH)(bpy)_2]^{2+}$	1.57	0.08	−0.69	−1.62	−1.86	SCE	MeCN	$TBAPF_6$	[65]
$[Ru(C_6H_4NHNH)(py)_4]^{2+}$	1.33[a]	−0.48	−1.24			SCE	MeCN	$TBAPF_6$	[66]
$[Ru(C_6H_4NHNH)(NH_3)_4]^{2+}$		0.65	−0.73[b]			SCE	MeCN	H_3PO_4	[36]
$[Ru(4,5\text{-}(OMe)_2C_6H_2NHNH)(NH_3)_4]^{2+}$		0.32	−0.40[b]			SCE	MeCN	H_3PO_4	[36]
$[Ru(C_6H_4NHNH)(edta)]^{2-}$		0.74	−0.47[b]			NHE	H_2O (pH 4.7)	NaTFA	[37]
$Ru(C_6H_4NHNPh)(acac)_2$	1.60[a]	0.41	−1.05	−2.04[a]		SCE	MeCN	$TBAClO_4$	[114]
$Ru(C_6H_4NHNH)(acac)_2$	1.56[a]	0.38	−1.13	2.10[a]		SCE	MeCN	$TBAClO_4$	[114]
$[Ru(trpy)(3,5\text{-}{}^tBu_2C_6H_2O_2)(OH_2)]^{2+}$			0.31	−0.47		SCE	CH_2Cl_2	$TBAClO_4$	[101,106]
$[Ru(trpy)(4\text{-}ClC_6H_3O_2)(OH_2)]^{2+}$			0.60	−0.14		SCE	CH_2Cl_2	$TBAClO_4$	[106]
$[Ru(trpy)(C_6H_4ONH)Cl]^+$	1.45	1.26	−0.26	−1.07	−1.79	SCE	MeCN	$TBAClO_4$	[35]
$[Ru(trpy)(C_6H_4ONH)Cl]^+$	1.41	1.17	−0.21	−1.02		Ag/AgCl	acetone	$TBAPF_6$	[100]
$[Ru(trpy)(4\text{-}{}^tBuC_6H_3ONH)Cl]^+$	1.38	1.19	−0.27	−1.05		Ag/AgCl	acetone	$TBAPF_6$	[100]
$[Ru(trpy)(4\text{-}{}^tBuC_6H_3ONH)(OAc)]^+$	1.28	1.13	−0.23	−1.01		Ag/AgCl	acetone	$TBAPF_6$	[100]
$[Ru(trpy)(5\text{-}MeC_6H_3ONH)(OAc)]^+$	1.26	1.14	−0.22	−0.86		Ag/AgCl	acetone	$TBAPF_6$	[100]
$[Ru(trpy)(4\text{-}MeC_6H_3ONH)(OAc)]^+$	1.26	1.14	−0.21	−1.01		Ag/AgCl	acetone	$TBAPF_6$	[100]
$[Ru(trpy)(C_6H_4ONH)(OAc)]^+$		1.15	−0.17	−0.98		Ag/AgCl	acetone	$TBAPF_6$	[100]
$[Ru(trpy)(5\text{-}ClC_6H_3ONH)(OAc)]^+$		1.26	−0.07	−0.89		Ag/AgCl	acetone	$TBAPF_6$	[100]
$[Ru(trpy)(4\text{-}ClC_6H_3ONH)(OAc)]^+$		1.38	−0.06	−0.89		Ag/AgCl	acetone	$TBAPF_6$	[100]
$[Ru(trpy)(4,6\text{-}{}^tBu_2C_6H_2ONPh)(OAc)]^+$	1.45	1.27	−0.19	−1.02		Ag/AgCl	acetone	$TBAPF_6$	[100]
$[Ru(trpy)(4,6\text{-}{}^tBu_2C_6H_3ON(2\text{-}CF_3Ph)(OAc)]^+$	1.50	1.38	−0.14	−1.02		Ag/AgCl	acetone	$TBAPF_6$	[100]
$[Ru(trpy)(C_6H_4NHNH)Cl]^+$	0.94	1.32	−0.54	−0.70	−1.27	SCE	MeCN	$TBAClO_4$	[35]
$[Ru(trpy)(C_6H_4NHNH)Cl]^+$	0.96					Ag/AgCl	MeCN	$TBAPF_6$	[99]
$[Ru(trpy)(C_6H_4NHNH)(NCMe)]^{2+}$	1.42					Ag/AgCl	MeCN	$TBAPF_6$	[99]
$[Ru(NH_2\text{–}L)(3,5\text{-}{}^tBu_2C_6H_2O_2)]^{2+}$			0.20	−0.77		SCE	CH_2Cl_2	$TBAPF_6$	[104]
$Ru(NPh\text{–}bpa)(3,5\text{-}{}^tBu_2C_6H_2O_2)$		0.72[a]	−0.37	−1.18		SCE	DME	$TBAClO_4$	[103]
$[Ru_2(btpyan)(3,6\text{-}{}^tBu_2C_6H_2O_2)_2(OH)_2]^{2+}$	0.43	0.35	−0.47	−0.56		Ag/AgCl	MeOH		[22,23]
$Ru_2(btpyan)(3,6\text{-}{}^tBu_2C_6H_2O_2)_2(O)_2$	0.30	0.40	−0.43	−0.68		Ag/AgCl	MeOH		[22,23]
$[Ru_2(btpyxa)(3,6\text{-}{}^tBu_2C_6H_2O_2)_2(Cl)_2]^{2+}$		0.13	0.09	−0.75		SCE	CH_2Cl_2	$TBAClO_4$	[130]
Class C									
$Ru(3,5\text{-}{}^tBu_2C_6H_2O_2)(PPh_3)_2(CO)Cl$	0.42	−0.55				SCE	MeCN	$TBAClO_4$	[73]
$Ru(Cl_4C_6O_2)(PPh_3)_2(CO)Cl$	0.87	−0.05				SCE	MeCN	$TBAClO_4$	[73]
$Ru(Cl_4C_6O_2)(PPh_3)_2(CO)H$	1.00	0.15				SCE	MeCN	$TBAClO_4$	[73]
$[Ru(C_6H_4O_2)(NH_3)_4]^+$		0.23	−0.70			Ag/AgCl	H_2O (pH 7)	KCl	[90]
$Ru(4\text{-}CO_2C_6H_3O_2)(NH_3)_4$		0.32	−0.65			Ag/AgCl	H_2O (pH 7)	KCl	[90]I
		0.32	−0.69			Ag/AgCl	H_2O (pH 7)	KCl	[91]
$[Ru(4\text{-}OMeC_6H_3O_2)(NH_3)_4]^+$		0.22	−0.70			Ag/AgCl	H_2O (pH 7)	KCl	[90]
$[Ru(4\text{-}C_2H_4NH_2C_6H_3O_2)(NH_3)_4]^+$		0.20	−0.35	−0.80		Ag/AgCl	H_2O (pH 7)	KCl	[91]
$[Ru(4\text{-}CH(OH)CH_2NH_2C_6H_3O_2)(NH_3)_4]^+$		0.24	−0.35	−0.70		Ag/AgCl	H_2O (pH 7)	KCl	[91]
$[Ru(C_6H_4O_2)(edta)]^{3-}$		0.40				NHE	H_2O (pH 7.5)	NaTFA	[127]
			−0.10				H_2O (pH 10)	NaTFA	[94]
$[Ru(4\text{-}CO_2C_6H_3O_2)(edta)]^{4-}$		0.46				NHE	H_2O (pH 7.5)	NaTFA	[127]
			−0.06				H_2O (pH 10)	NaTFA	[94]
$[Ru(3,5\text{-}(SO_3)_2C_6H_2O_2)(edta)]^{5-}$		0.59				NHE	H_2O (pH 7.5)	NaTFA	[127]
		0.02				NHE	H_2O (pH 10)	NaTFA	[94]
$[Ru(4\text{-}C_2H_4NH_2C_6H_3O_2)(edta)]^{3-}$			−0.12			NHE	H_2O (pH 10)	NaTFA	[94]
$[Ru(C_6H_4ONH)(bpy)_2]^+$		1.48	0.05	−0.70		SCE	MeCN	$TBAPF_6$	[66]
$[Ru(4,6\text{-}{}^tBu_2C_6H_2ONPh)(bpy)_2]^+$		1.22	−0.42	−1.29		NHE	H_2O (pH 10)	NaTFA	[38]
$[Ru(trpy)(4\text{-}ClC_6H_3O_2)(PPh_3)]^+$			0.76	−0.09		SCE	CH_2Cl_2		[96]
$Ru(trpy)(3,5\text{-}{}^tBu_2C_6H_2O_2)Cl$			0.84	−0.37	−1.26	Fc/Fc^+	CH_2Cl_2	$TBABF_4$	[97]
$Ru(trpy)(3,5\text{-}{}^tBu_2C_6H_2O_2)Cl$		0.77[a]	−0.23	−1.07	−2.20[a]	Fc/Fc^+	MeCN	$TBABF_4$	[97]
$Ru(trpy)(3,5\text{-}{}^tBu_2C_6H_2O_2)Cl$			0.89	−0.31	−1.22	Fc/Fc^+	CH_2Cl_2	$TBAClO_4$	[98]
$[Ru(trpy)(3,5\text{-}{}^tBu_2C_6H_2O_2)(NH_3)]^+$			0.34	−0.46		SCE	CH_2Cl_2		[101]
$Ru(trpy)(C_6H_4O_2)(OAc)$			−0.21	−1.07		Fc/Fc^+	CH_2Cl_2	$TBABF_4$	[97]
$Ru(trpy)(Cl_4C_6O_2)(OAc)$			0.19	−0.80		Fc/Fc^+	CH_2Cl_2	$TBABF_4$	[97]
$Ru(trpy)(4\text{-}NO_2C_6H_3O_2)(OAc)$			0.18	−0.78		Fc/Fc^+	CH_2Cl_2	$TBABF_4$	[97]
$Ru(trpy)(3,5\text{-}{}^tBu_2C_6H_2O_2)(OAc)$		0.82[a]	−0.38	−1.24		Fc/Fc^+	CH_2Cl_2	$TBABF_4$	[97]
$Ru(trpy)(3,5\text{-}{}^tBu_2C_6H_2O_2)(OAc)$			0.18	−0.68		SCE	CH_2Cl_2	$TBAClO_4$	[41]
$Ru(trpy)(4\text{-}{}^tBuC_6H_3O_2)(OAc)$			0.27	−0.57		SCE	CH_2Cl_2	$TBAClO_4$	[41]

Table 5 (*Continued*)

Complex	$E_{1/2}$	$E_{1/2}$	$E_{1/2}$	$E_{1/2}$	$E_{1/2}$		Solvent	Counterelectrolyte	Ref.
Ru(trpy)(4-$ClC_6H_3O_2$)(OAc)			0.44	−0.45		SCE	CH_2Cl_2	$TBAClO_4$	[41]
Ru(trpy)(3,5-$Cl_2C_6H_2O_2$)(OAc)			0.57	−0.37		SCE	CH_2Cl_2	$TBAClO_4$	[41]
Ru(trpy)($Cl_4C_6O_2$)(OAc)			0.67	−0.28		SCE	CH_2Cl_2	$TBAClO_4$	[41]
[Ru(trpy)(3,6-$^tBu_2C_6H_2O_2$)(CO)]$^+$			0.33	−0.72	−1.91[a]	Fc/Fc^+	CH_2Cl_2	$TBAPF_6$	[122]
[Ru(trpy)(3,5-$^tBu_2C_6H_2O_2$)(CO)]$^+$			0.49	−0.58		$Ag/AgNO_3$	CH_2Cl_2	$TBAClO_4$	[102]
[Ru(trpy)(3,5-$^tBu_2C_6H_2O_2$)(DMSO)]$^+$			0.65	−0.32		SCE	CH_2Cl_2	$TBAPF_6$	[122]
Class D									
Cp*Ru($C_6H_4O_2$)(NO)	0.42	−1.21				Fc/Fc^+	MeCN	$TBAClO_4$	[131]
Cp*Ru(4-$MeC_6H_3O_2$)(NO)	0.29	−1.27				Fc/Fc^+	MeCN	$TBAClO_4$	[131]
Cp*Ru(4-$^tBuC_6H_3O_2$)(NO)	0.32	−1.20				Fc/Fc^+	MeCN	$TBAClO_4$	[131]
Cp*Ru(4-$FC_6H_3O_2$)(NO)	0.47	−1.23				Fc/Fc^+	MeCN	$TBAClO_4$	[131]
Cp*Ru(4-$ClC_6H_3O_2$)(NO)	0.40	−1.27				Fc/Fc^+	MeCN	$TBAClO_4$	[131]
Cp*Ru($Cl_4C_6O_2$)(NO)	0.75	−1.04				Fc/Fc^+	MeCN	$TBAClO_4$	[131]
Cp*Ru($Br_4C_6O_2$)(NO)	0.77	−1.07				Fc/Fc^+	MeCN	$TBAClO_4$	[131]
Ru($Cl_4C_6O_2$)(PPh_3)$_2$(CO)$_2$	1.76	0.65				SCE	CH_2Cl_2	$TBAPF_6$	[68]
Ru($Br_4C_6O_2$)(PPh_3)$_2$(CO)$_2$	1.70	0.66				SCE	CH_2Cl_2	$TBAPF_6$	[68]
Ru($C_6H_4O_2$)(PPh_3)$_2$(CO)$_2$	0.791	−0.388				Fc/Fc^+	CH_2Cl_2	$TBAPF_6$	[79]
Ru(4-$MeC_6H_3O_2$)(PPh_3)$_2$(CO)$_2$	0.676	−0.461				Fc/Fc^+	CH_2Cl_2	$TBAPF_6$	[79]
Ru($C_6H_4O_2$)(PPh_3)$_2$(CO)$_2$	1.58	0.55				Ag/AgCl	CH_2Cl_2		[81]
Ru($C_6H_4O_2$)(CO)$_2$(py)$_2$	0.860	−0.132				Fc/Fc^+	CH_2Cl_2	$TBAPF_6$	[79]
Ru($C_6H_4O_2$)(CO)(py)$_3$	0.589	−0.318				Fc/Fc^+	CH_2Cl_2	$TBAPF_6$	[79]
Ru($C_6H_4O_2$)(CO)$_2$(PPh_3)(py)	1.66[a]	0.68				Ag/AgCl	CH_2Cl_2		[81]
Ru($C_6H_4O_2$)(bpy)$_2$	1.65[a]	0.56	−0.33	−1.72		SCE	MeCN	$TBAPF_6$	[66]
[c]Ru(3,5-$^tBu_2C_6H_2O_2$)(bpy)$_2$	1.49[a]	0.39	−0.51	−1.75		SCE	CH_2ClCH_2Cl	$TBAPF_6$	[86]
[c]Ru($Cl_4C_6O_2$)(bpy)$_2$	1.68[a]	0.88	0.02	−1.69		SCE	CH_2ClCH_2Cl	$TBAPF_6$	[86]
Ru($C_6H_4O_2$)(py)$_4$	1.52[a]	0.59	−0.34			SCE	MeCN	$TBAPF_6$	[66]
[c]Ru(4-$^tBuC_6H_3O_2$)(py)$_4$	1.79[a]	0.40	−0.60			SCE	CH_2ClCH_2Cl	$TBAPF_6$	[86]
[c]Ru($Cl_4C_6O_2$)(py)$_4$		0.94	−0.09				CH_2ClCH_2Cl	$TBAPF_6$	[86]
[Ru($C_6H_4O_2$)(CO)$_2$(PPh_3)Cl]$^-$	1.41[a]	0.39				Ag/AgCl	CH_2Cl_2		[81]
[Ru($C_6H_4O_2$)(CO)$_2$(PPh_3)Br]$^-$	1.44[a]	0.38				Ag/AgCl	CH_2Cl_2		[81]
[Ru($C_6H_4O_2$)(CO)$_2$(PPh_3)I]$^-$	1.35[a]	0.34				Ag/AgCl	CH_2Cl_2		[81]
[Ru($Cl_4C_6O_2$)(CN)(CO)$_2$(PPh_3)]$^-$	1.52[a]	0.44				SCE	CH_2Cl_2	$TBAPF_6$	[77]
[Ru($Cl_4C_6O_2$)(CN)(CO)$_2$(P(OPh)$_3$)]$^-$	1.67[a]	0.51				SCE	CH_2Cl_2	$TBAPF_6$	[77]
Ru($Cl_4C_6O_2$)(NCMe)(CO)$_2$(PPh_3)	1.65[a]	0.79				SCE	CH_2Cl_2	$TBAPF_6$	[77]

[a] Irreversible process.
[b] Irreversible $2e^-$ $2H^+$ PCET process.
[c] Potentials have been corrected from literature values to account for mathematical errors in converting between reference electrodes.

In a related study by Masui et al., the substituent effect on the NIL ligand was investigated for the complexes $[Ru(NIL)(bpy)_2]^n$ where NIL = 4-$NO_2C_6H_3NHNH$, 4,5-$Cl_2C_6H_2NHNH$, C_6H_4NHNH, 4,5-$Me_2C_6H_2NHNH$, 4,5-$(OMe)_2C_6H_2NHNH$, 4,5-$(NH_2)_2C_6H_2NHNH$ with some of these systems investigated in a variety of redox states, i.e., n = 2+, 1+ or 0 [65]. These systems show one metal and two NIL based redox couples (*cf.*, Fig. 3) all showing a linear dependence on the Hammett $\Sigma\sigma_p$ parameters where an anodic shift is observed with increasing electron withdrawing ability of the NIL ligand (Table 5). In contrast, the Ru–NIL based electronic transitions were found to show only a weak dependence on $\Sigma\sigma_p$. This has been attributed to differences in reorganization energies as discussed in the introduction [62]. The lack of charge transfer character here is consistent with resonance Raman studies, and the narrow bandwidths observed for these transitions [25,65].

An in-depth EPR analysis of the Class C N-substituted Ru–NIL species $[Ru(4,6\text{-}^tBu_2C_6H_2ONPh)(bpy)_2]^+$ was recently reported by Ye et al. where the resonance form Ru^{II}–NIL$^\bullet$ was found to be predominant (Scheme 5) [38]. At room temperature a g_{iso} value of 2.0049 (CH_2Cl_2) was reported which is very similar to the free semiquinone g_{iso} value of 2.0061 (DMSO) [89]. At low temperature a large Ru hyperfine coupling was observed attributed to efficient spin polarization made possible by the strong Ru($d\pi$)–NIL(π^*) electronic coupling consistent with the large Δg value of 0.0665. This predominance of the Ru^{II}–NIL$^\bullet$ resonance form in Class C ruthenium polypyridyl systems is consistent with previous studies [65,66,86].

In contrast, Salmonsen et al. have shown that by substituting the pyridyl co-ligands with a more basic ligand set, the resonance can be pushed in favor of the Ru^{III}–NIL^{Red} electronic configuration for Class C systems due to the relatively easier oxidation of the metal center [42]. The complex Ru(4-(CH_2CO_2)–$C_6H_3O_2$)$(NH_3)_4$, which has no net formal charge at basic pH due to deprotonation of the carboxy group, displayed a low temperature EPR spectrum typical of Ru^{III} ($g_\perp$ = 2.722 and $g_{||}$ = 1.889), thus implying the resonance structure Ru^{III}–NIL^{Red}. Similar behavior was observed by da Silva et al. for the Class C systems $[Ru(4\text{-R-}C_6H_3O_2)(NH_3)_4]^+$ (R = H, CO_2H) [90]. Interestingly, upon oxidation of the Class C systems containing the dopamine, noradrenaline or isoproterenol ligands to their Class B analogues $[Ru(4\text{-R-}C_6H_3O_2)(NH_3)_4]^{2+}$ (R = $C_2H_4NH_2$, $CH(OH)CH_2NH_2$, $CH(OH)CH_2NHCH(CH_3)_2$, respectively) the Ru^{II} oxidation state becomes more favorable, i.e., Ru^{II}–NIL^{Ox} is preferred over the Ru^{III}–NIL$^\bullet$ resonance form (Scheme 6) [91]. This was again proven to be the case by Lever and Gorelsky for the complexes $[Ru(4,5\text{-}R_2C_6H_2NHNH)(NH_3)_4]^{2+}$ (R = H, Cl and OMe) by examining the percentage mixing of the Ru(t_{2g}) and NIL(π^*/π) orbitals [36,92]. For all of these Class B Ru^{II}–NIL^{Ox} complexes, the NIL was observed to be a much better π-acceptor, i.e. increased Ru → NIL backbonding, when the central Ru was made more electron rich using the tetraammine ligand set in place of the bis-bipyridyl ligand set. One-electron oxidation of the Class B systems was clearly ascribed to the $Ru^{III/II}$ couple via spectroelectrochemical EPR analysis in aqueous acidic media (Table 3) [36]. An irreversible two-electron, two-proton-coupled reduction process is observed at pH 1 over a wide potential range depending on the electron donating/withdrawing nature of the NIL substituent (−0.40 to −0.86 V *vs.* SCE) giving rise to formation of the protonated Ru^{II}–H_2NIL^{Red} species $[Ru(4,5\text{-}R_2C_6H_2NH_2NH_2)(NH_3)_4]^{3+}$. In this case, the one-electron reduction of the mono-protonated mono-reduced species Ru^{II}–(H)NIL$^\bullet$ is easier than the one-electron reduction of the starting Ru^{II}–NIL^{Ox} complex, a process which is well documented for

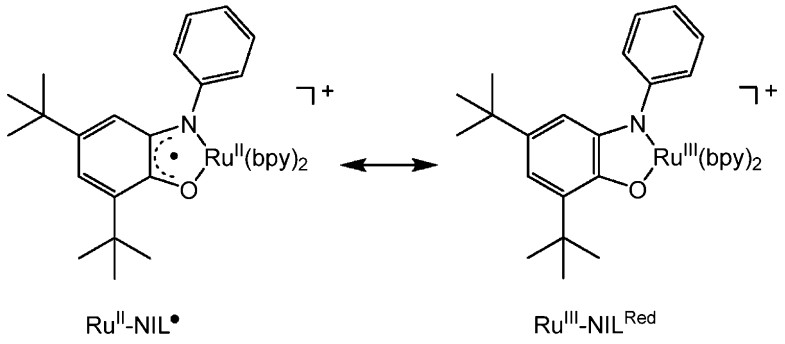

Scheme 5. Resonance forms of the Class C species $[Ru(4,6\text{-}^tBu_2C_6H_2ONPh)(bpy)_2]^+$ studied by Ye et al. via EPR spectroscopy (see Table 3 for EPR data).

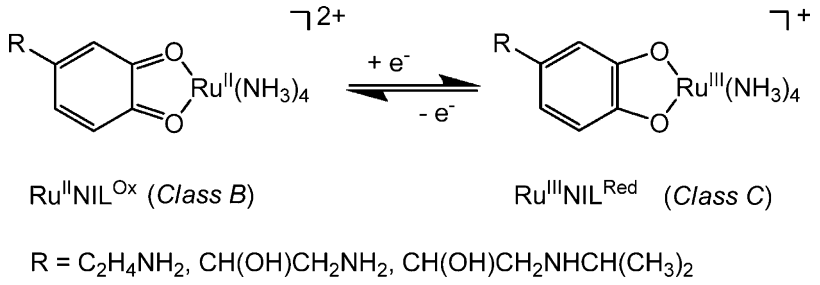

Scheme 6.

the free quinone ligand [93]. The edta analogue studied by Rein et al. $[Ru(C_6H_4NHNH)(edta)]^{2-}$ likewise is shown to adopt the Ru^{II}–NIL^{Ox} resonance form typical of Class B systems, even with such an electron rich metal center [37]. Again, an irreversible two-electron, two-proton-coupled reduction process is observed for the latter complex in acidic media. Such pH dependent redox chemistry correlates well with the different redox states isolated under neutral/aerobic and basic/anaerobic conditions [94].

The very basic edta ligand of the Class C complexes $[Ru^{III}(NIL)(edta)]^{n-}$ where NIL is $C_6H_4O_2$, $4\text{-}CO_2HC_6H_3O_2$ and $3,5\text{-}(SO_3Na)_2C_6H_2O_2$ makes these systems comparable to their tetraammine analogues and similar redox chemistry has been reported [95]. A one-electron ligand-based oxidation process was reported in the range 0.40–0.59 V *vs.* NHE for these systems (pH 7–7.5). However, the $Ru^{III/II}$ metal based reduction occurred at much more negative potentials (*ca.* −0.5 V *vs.* NHE) which led to dissociation of the NIL even under weakly basic conditions indicating the instability of such electron rich Class D complexes in the presence of a proton source. Analogous behavior has also been reported for the Ru(edta) dopamine and L-dopa complexes $[Ru^{III}(4\text{-}C_2H_4NH_2C_6H_4O_2)(edta)]^{3-}$ and $[Ru^{III}(4\text{-}CH_2CH(CO_2)NH_2C_6H_4O_2)(edta)]^{4-}$, respectively [94].

5. Ru(trpy)(NIL)L

5.1. L = phosphine

The treatment of $Ru(trpy)(PPh_3)Cl_2$ with catecholate and the oxidant $AgClO_4$ affords the Class C complex $[Ru(trpy)(4\text{-}ClC_6H_3O_2)(PPh_3)][ClO_4]$ which displays a reduction and a oxidation event at −0.09 and 0.76 V vs. SCE, respectively [96]. The chemical reduction of $[Ru(trpy)(4\text{-}ClC_6H_3O_2)(PPh_3)][ClO_4]$ with $Na_2S_2O_4$ yields the neutral Class D species $Ru(trpy)(4\text{-}ClC_6H_3O_2)(PPh_3)$. Both $[Ru(trpy)(4\text{-}ClC_6H_3O_2)(PPh_3)][ClO_4]$ and its one-electron reduced derivative $Ru(trpy)(4\text{-}ClC_6H_3O_2)(PPh_3)$ are characterized by X-ray crystallography. This is a rare example of a Ru–NIL system crystallographically characterized in two oxidation states. The C–O distances in $[Ru(trpy)(4\text{-}ClC_6H_3O_2)(PPh_3)][ClO_4]$ (1.289(7) and 1.304(7) Å) are shorter than in the $Ru(trpy)(4\text{-}ClC_6H_3O_2)(PPh_3)$ (1.320(10) and 1.343(9) Å) derivatives. The XPS analysis of $[Ru(trpy)(4\text{-}ClC_6H_3O_2)(PPh_3)][ClO_4]$ and $Ru(trpy)(4\text{-}ClC_6H_3O_2)(PPh_3)$ shows similar Ru binding energies of 280.3 and 280.7 eV, respectively. This small change in Ru binding energies is consistent with a ligand-based oxidation, especially when compared to the $Ru(bpy)_2Cl_2^{0/+}$ system where the Ru^{II} and the Ru^{III} derivative display binding energy of 279.9 eV and 281.9 eV, respectively (Table 6). The Class C species $[Ru(trpy)(4\text{-}ClC_6H_3O_2)(PPh_3)][ClO_4]$ is EPR active and displays an isotropic signal at $g = 2.00$ in CH_2Cl_2 at room temperature. Collectively, the experimental evidence indicates a Ru^{II} oxidation state in both species with the Class C compound $[Ru(trpy)(4\text{-}ClC_6H_3O_2)(PPh_3)][ClO_4]$ exhibiting predominately Ru^{II}–$NIL^{\bullet}$ character. The $[Ru(trpy)(4\text{-}ClC_6H_3O_2)(PPh_3)]^{0/+}$ system containing both an electron withdrawing NIL and a strong field phosphine co-ligand displays a predominately ligand localized redox reactivity. Now we turn to the more prevalent and intriguing cases of ambiguous or non-integer oxidation state assignments in Ru–NIL complexes with terpyridine co-ligands.

5.2. L = acetate or chloride

The ability to modulate the electron distribution within the Ru–NIL framework by altering the electron withdrawing abil-

Table 6
XPS data for Ru–NIL complexes.

Complex	Ru (eV)	Ref.
$[Ru^{II}(en)_3](ZnCl_4)$	279.5	[132]
$Ru^{II}(bpy)_2Cl_2$	279.9	[133]
$Ru(trpy)(3,5\text{-}^tBu_2C_6H_2O_2)(OAc)$	280.3	[106,41]
$Ru(trpy)(4\text{-}ClC_6H_3O_2)(PPh_3)$	280.3	[96]
$[Ru(trpy)(3,5\text{-}^tBu_2C_6H_2O_2)(NH_3)](ClO_4)$	280.4	[101]
$[Ru(trpy)(4\text{-}ClC_6H_3O_2)(PPh_3)](ClO_4)$	280.7	[96]
$[Ru(trpy)(3,5\text{-}^tBu_2C_6H_2O_2)(NH_3)](ClO_4)_2$	281.2	[101]
$[Ru(trpy)(3,5\text{-}^tBu_2C_6H_2O_2)(OH_2)](ClO_4)_2$	281.3	[106,129]
$[Ru^{III}(bpy)_2Cl_2]Cl$	281.9	[133]
$[Ru^{III}(NH_3)_6]Cl_3$	282.1	[132]

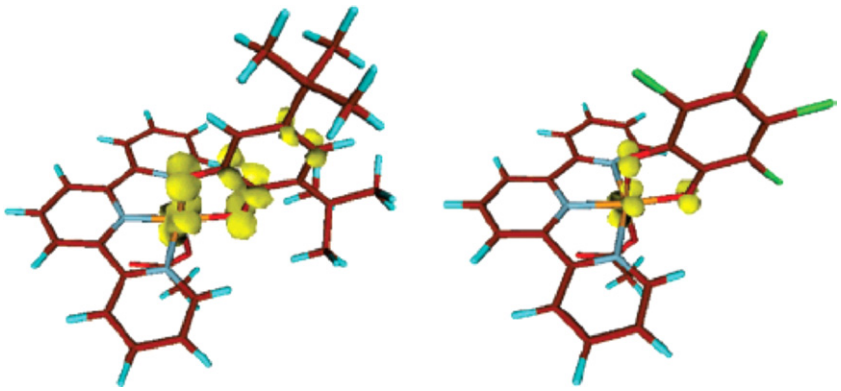

Fig. 5. Spin density plots of Ru(trpy)(3,5-$^{t}Bu_2C_6H_2O_2$)(OAc) (left) and Ru(trpy)($Cl_4C_6O_2$)(OAc) (right). This figure was reproduced from Ref. [41] with permission of the copyright holders.

ity of the NIL is clearly illustrated by Tanaka and co-workers with a family of Ru(trpy)(NIL)(OAc) complexes [41]. The Class C Ru(trpy)(NIL)(OAc) complexes (where NIL = 3,5-$^{t}Bu_2C_6H_2O_2$, 4-$^{t}BuC_6H_3O_2$, 4-$ClC_6H_3O_2$, 3,5-$Cl_2C_6H_2O_2$, $Cl_4C_6O_2$) all display an intermediate electronic structure with contributions from the Ru^{II}–NIL$^{\bullet}$ and Ru^{III}–NIL^{Red} resonance states. A thorough EPR study of this family of compounds reveals an increasing contribution from the Ru^{III}–NIL^{Red} state as the electron withdrawing ability of the NIL substituents is increased (Table 3). The UV–vis spectroscopy also indicates a shift in electron distribution over the Ru–NIL fragment upon altering the NIL. The UV–vis spectra of this series of complexes displays a decrease in molar extinction coefficients as the number of electron withdrawing substituents is increased. DFT calculations corroborate these experimental findings, showing an increased spin density on the ruthenium center in Ru(trpy)($Cl_4C_6O_2$)(OAc) (Ru^{III}–NIL^{Red}) compared to Ru(trpy)(3,5-$^{t}Bu_2C_6H_2O_2$)(OAc) (Ru^{II}–NIL$^{\bullet}$) (Fig. 5).

The [Ru(trpy)(NIL)Cl]^{n} systems show rich redox chemistry, but the electronic structure of the Class B species (n = +1) is not without ambiguity. Bhattacharya and Tanaka have independently reported the Class C compound Ru(trpy)(3,5-$^{t}Bu_2C_6H_2O_2$)(Cl) which is satisfactorily assigned as Ru^{II}–NIL$^{\bullet}$ [41,97,98]. The one-electron oxidized product [Ru(trpy)(3,5-$^{t}Bu_2C_6H_2O_2$)(Cl)]$^{+}$, however, was assigned differently by the two groups. Bhattacharya assigns the oxidation product as metal based (Ru^{III}–NIL$^{\bullet}$), whereas Tanaka suggests the ligand-based oxidation (Ru^{II}–NIL^{Ox}). Tanaka's assign-

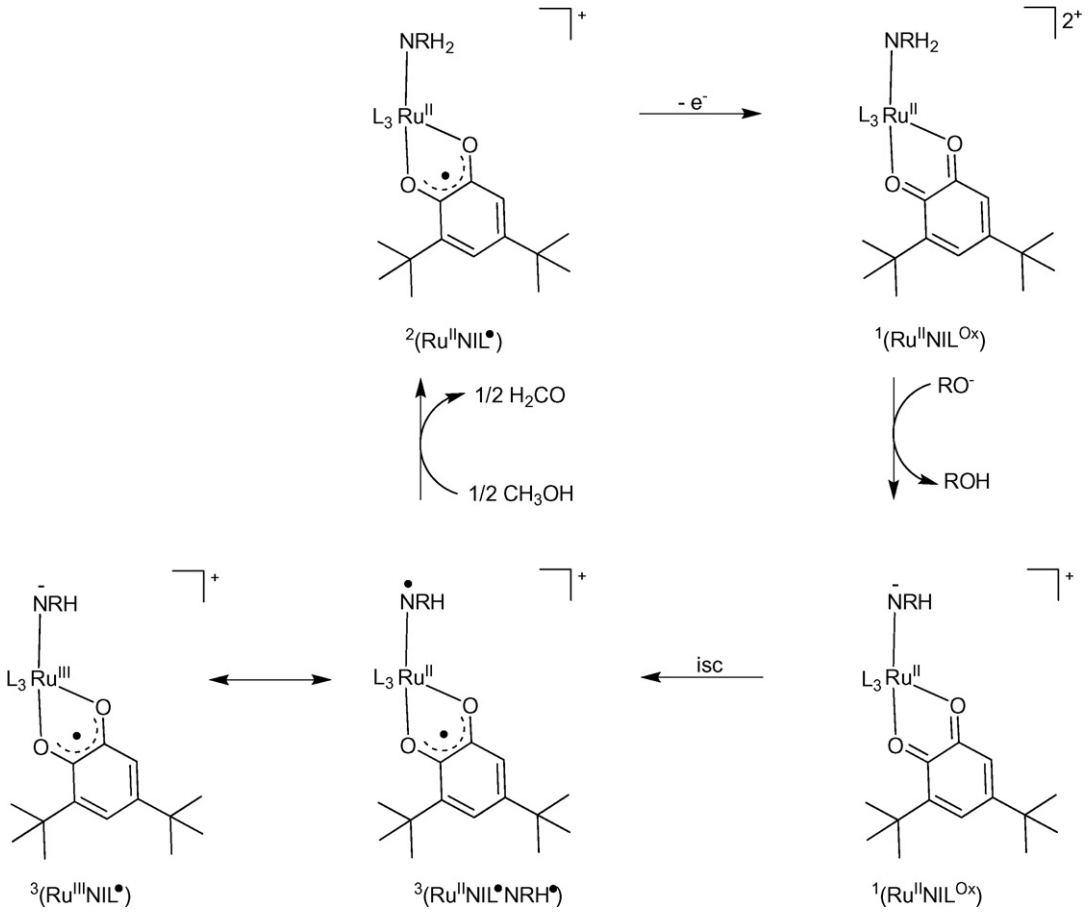

Scheme 7. Proposed catalytic scheme for alcohol oxidation based on new DFT calculations.

ment is more likely, however, with a distinct contribution from the Ru^{III}–NIL• resonance form based on recent theoretical analysis of the isoelectronic hydroxy species by Tsai et al. [39]. In a related study, the complexes [Ru(trpy)(NIL)Cl]$^+$ (where NIL = C_6H_4ONH and C_6H_4NHNH) were reported [35,99]. These Class B compounds are described as displaying predominately Ru^{III}–NIL• character with only a minor contribution from the Ru^{II}–NIL^{Ox} state [35]. Crystallographic studies of these compounds reveal bond distances somewhere between the expected distances for an NIL• and NIL^{Ox} redox state, suggesting an intermediate electronic structure. The DFT calculations for [Ru(trpy)(C_6H_4ONH)Cl]$^+$ and [Ru(trpy)(C_6H_4NHNH)Cl]$^+$ reveal a delocalized ground state with the Ru(dπ) orbitals extensively mixed with the NIL(π/π^*) orbitals and the Cl(π) orbitals. The authors prepared both the one-electron oxidized Class A species [Ru(trpy)(C_6H_4ONH)Cl]$^{2+}$ and [Ru(trpy)(C_6H_4NHNH)Cl]$^{2+}$ and the one-electron reduced Class C species Ru(trpy)(C_6H_4ONH)Cl and Ru(trpy)(C_6H_4NHNH)Cl. The authors' assign the Class A and Class C species as Ru^{IV}–NIL• and Ru^{II}–NIL•, respectively. This unusual solely metal based redox activity is debatable, and a detailed study of [Ru(trpy)(NIL)Cl]^n with contrary interpretation is forthcoming [100].

Examination of the Class C compounds [Ru(trpy)(3,5-^{t}Bu$_2$C$_6$H$_2$O$_2$)L]^n (L = CO, NH_3, n = +1; L = Cl and OAc, n = 0) illustrates the influence ancillary ligands have on the metal orbital energies [97,101,102]. UV–vis spectroscopy clearly demonstrates that altering the co-ligand from a strong field carbonyl ligand to a weak field chloride ligand decreases the energy gap of the MLCT transition,[4] as well as increasing the Ru(dπ)–NIL(π^*) overlap. The [Ru(trpy)(3,5-^{t}Bu$_2$C$_6$H$_2$O$_2$)(CO)]$^+$ compound displays a CT band at 644 nm (4390 cm^{-1} M^{-1}), whereas the [Ru(trpy)(3,5-^{t}Bu$_2$C$_6$H$_2$O$_2$)(NH_3)]$^+$ compound displays a CT band at 854 nm (13 000 cm^{-1} M^{-1}). This trend is continued with the chloride and acetate analogs which display bands at 875 (16 900 cm^{-1} M^{-1}) and 883 (18 600 cm^{-1} M^{-1}), respectively.

5.3. L = amine

The Class C species [Ru(trpy)(3,5-^{t}Bu$_2$C$_6$H$_2$O$_2$)(NH_3)]$^+$ and the one-electron oxidized Class B derivative [Ru(trpy)(3,5-^{t}Bu$_2$C$_6$H$_2$O$_2$)(NH_3)]$^{2+}$ were prepared and characterized by a variety of spectroscopic techniques. The paramagnetic Class C species [Ru(trpy)(3,5-^{t}Bu$_2$C$_6$H$_2$O$_2$)(NH_3)]$^+$ displays a broad isotropic signal (g = 2.008) in its EPR spectrum and is assigned as Ru^{II}NIL• [80]. Since [Ru(trpy)(3,5-^{t}Bu$_2$C$_6$H$_2$O$_2$)(NH_3)]$^+$ and [Ru(trpy)(3,5-^{t}Bu$_2$C$_6$H$_2$O$_2$)(NH_3)]$^{2+}$ displayed binding energies for the Ru $3d_{5/2}$ of 280.4 and 281.2 eV, respectively, the authors assigned the latter as a Ru^{III}–NIL• species (Table 6). Is the electronic structure of [Ru(trpy)(3,5-^{t}Bu$_2$C$_6$H$_2$O$_2$)(NH_3)]$^{2+}$ actually Ru^{III}–NIL•? Our preliminary DFT calculations in CH_2Cl_2 suggest that the singlet Ru^{II}–NIL^{Ox} is 6.29 kcal/mol lower in energy than the triplet Ru^{III}–NIL• state [75]. Various spectroscopic properties (including the absorption spectrum) of this species are similar to those of [Ru(trpy)(3,5-^{t}Bu$_2$C$_6$H$_2$O$_2$)(OH_2)]$^{2+}$, which was also originally assigned as a Ru^{III}–NIL• species based on the XPS data. However, our recent study indicated that [Ru(trpy)(3,5-^{t}Bu$_2$C$_6$H$_2$O$_2$)(OH_2)]$^{2+}$ is a Ru^{II}–NIL^{Ox} species (see the L = OH_2 section).

The complex [Ru(trpy)(3,5-^{t}Bu$_2$C$_6$H$_2$O$_2$)(NH_3)]$^{n+}$ (n = 1, 2), containing both a protic ammine ligand and a redox-active NIL, is poised to display interesting redox-induced reactivity and indeed the complex [Ru(trpy)(3,5-^{t}Bu$_2$C$_6$H$_2$O$_2$)(NH_3)]$^{2+}$ catalyzes the electrochemical oxidation of alcohols. Although a detailed mechanism of alcohol oxidation by the complex remains unclear, treatment of methanol solutions of [Ru(trpy)(3,5-^{t}Bu$_2$C$_6$H$_2$O$_2$)(NH_3)]$^{2+}$ with 1 equiv of base (^{t}BuOK) was found to regenerate the [Ru(trpy)(3,5-^{t}Bu$_2$C$_6$H$_2$O$_2$)(NH_3)]$^+$ species [101]. The oxidation of alcohol by [Ru(trpy)(3,5-^{t}Bu$_2$C$_6$H$_2$O$_2$)(NH_3)]$^{2+}$ presumably proceeds through the deprotonation of the ammine ligand to afford the amido species [Ru(trpy)(3,5-^{t}Bu$_2$C$_6$H$_2$O$_2$)(NH_2)]$^+$, the Ru amido species undergoes intramolecular electron transfer to form the aminyl radical [Ru(trpy)(3,5-^{t}Bu$_2$C$_6$H$_2$O$_2$)(NH_2•)]$^+$, and finally the conversion of the [Ru(trpy)(3,5-^{t}Bu$_2$C$_6$H$_2$O$_2$)(NH_2•)]$^+$ to [Ru(trpy)(3,5-^{t}Bu$_2$C$_6$H$_2$O$_2$)(NH_3)]$^+$ is coupled with the oxidation of the alcohol by H atom abstraction (see Scheme 7). Our DFT calculations on [Ru(trpy)(3,5-^{t}Bu$_2$C$_6$H$_2$O$_2$)(NH_2•)]$^+$ revealed a near equal spin density on the Ru and N centers (Fig. 6) which is indicative of equal contributions from the [Ru^{II}(trpy)(NIL•)(NH_2•)]$^+$ and [Ru^{III}(trpy)(NIL•)(NH_2)]$^+$ resonance forms in the ground state.

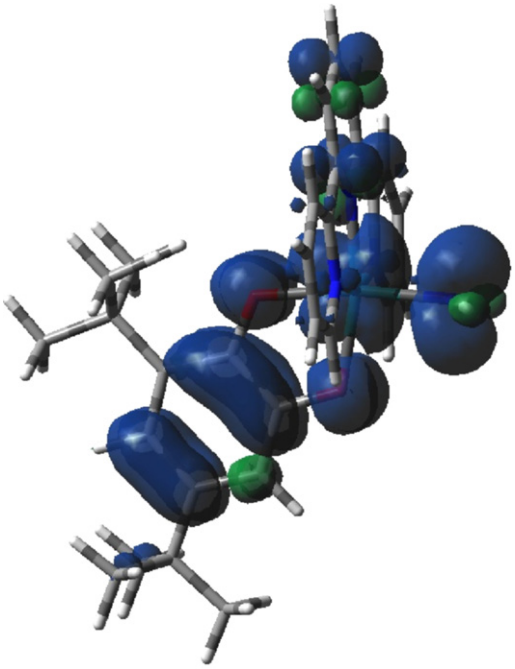

Fig. 6. Calculated spin density for [Ru(trpy)(3,5-^{t}Bu$_2$C$_6$H$_2$O$_2$)(NH_2)]$^+$ with the isodensity plotted at 0.001.

As mentioned above, the complex [Ru(trpy)(3,5-^{t}Bu$_2$C$_6$H$_2$O$_2$)(NH_3)]$^{n+}$ catalyzes the electrochemical oxidation of alcohols at mild conditions in basic alcohol solutions. The catalytic activity is, however, hampered by the formation of the inactive side product [Ru(trpy)(3,5-^{t}Bu$_2$C$_6$H$_2$O$_2$)(OCH_3)]$^+$ during the catalytic cycle [101]. To prevent the substitution of the ammine ligand by CH_3O^- in [Ru(trpy)(3,5-^{t}Bu$_2$C$_6$H$_2$O$_2$)(NH_3)]$^{n+}$, the trpy and ammine ligands were replaced with the tetradentate ligand bis(2-pyridylmethyl)-2-aminoethylamine (NH_2–L) [103,104]. The Class B compound [Ru(NH_2–L)(3,5-^{t}Bu$_2$C$_6$H$_2$O$_2$)](PF_6)$_2$ was assigned by the authors as being predominately Ru^{III}–NIL• in character. The Class C species [Ru(NH_2–L)(3,5-^{t}Bu$_2$C$_6$H$_2$O$_2$)]$^+$ was prepared electrochemically. The EPR spectrum of [Ru(NH_2–L)(3,5-^{t}Bu$_2$C$_6$H$_2$O$_2$)]$^+$ displays a g = 2.015 indicating a contribution from the Ru^{II}–NIL• electronic state. The oxidation state assignment of [Ru(NH_2–L)(3,5-^{t}Bu$_2$C$_6$H$_2$O$_2$)]$^{2+}$ may need to be reconsidered due to reasons similar to those mentioned for [Ru(trpy)(3,5-^{t}Bu$_2$C$_6$H$_2$O$_2$)(NH_3)]$^{2+}$. In fact, our preliminary DFT calculations in CH_2Cl_2 for [Ru(NH_2–L)(3,5-^{t}Bu$_2$C$_6$H$_2$O$_2$)]$^{2+}$ predict the closed-shell singlet state is ~5 kcal mol^{-1} lower than the triplet state, indicating this species is likely Ru^{II}–NIL^{Ox} [75].

The second generation [Ru(NH_2–L)(3,5-^{t}Bu$_2$C$_6$H$_2$O$_2$)](PF_6)$_2$ framework is more robust under catalytic conditions, displaying greater catalytic activity for the oxidation of alcohols than its predecessor [Ru(trpy)(3,5-^{t}Bu$_2$C$_6$H$_2$O$_2$)(NH_3)]$^{2+}$ (Scheme 7). The catalytically active species for both systems is likely an incipient aminyl radical which abstracts a hydrogen atom from the alcohol.

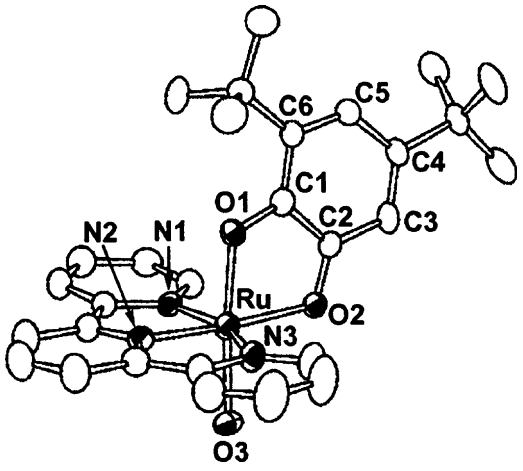

Fig. 7. Molecular structure of $[Ru(trpy)(3,5\text{-}^tBu_2C_6H_2O_2)(OH_2)]^{2+}$ with the hydrogen atoms omitted for clarity. This figure was reproduced from Ref. [106] with permission of the copyright holders.

The reactive nature of the aminyl radical prevents its detection. Experimental evidence for the aminyl radical was possible, however, with the complex $[Ru(NHPh\text{–}bpa)(3,5\text{-}^tBu_2C_6H_2O_2)]^+$ where NHPh–bpa = 2-(bis(2-pyridylmethyl)aminomethyl)anilido ligand. The anilido radical was characterized by EPR and XPS along with DFT calculations [103]. However, UV–vis-NIR spectra of this species, the deprotonated species and the further reduced species are quite complicated and a further theoretical study is needed to elucidate the nature of electronic transitions and the electron distribution over the (NHPh–bpa)–Ru–NIL and (•NPh–bpa)–Ru–NIL framework.

5.4. L = aqua

The first report of a Ru–NIL complex with an aqua ancillary ligand was that of $[Ru(trpy)(3,5\text{-}^tBu_2C_6H_2O_2)(OH_2)]^+$ by Bhattacharya [98]. The Class C species $[Ru(trpy)(3,5\text{-}^tBu_2C_6H_2O_2)(OH_2)]^+$ was the proposed product from the reaction of $Ru(trpy)(3,5\text{-}^tBu_2C_6H_2O_2)Cl$ with $AgClO_4$ [98]. Further investigation by Tanaka and co-workers proved the Ru(III) derivative $[Ru(trpy)(3,5\text{-}^tBu_2C_6H_2O_2)Cl]^+$ to be the major product in the latter reaction. The complex $[Ru(trpy)(3,5\text{-}^tBu_2C_6H_2O_2)(OH_2)]^{2+}$ was successfully prepared by treatment of $Ru(trpy)(3,5\text{-}^tBu_2C_6H_2O_2)(OAc)$ with a strong acid [105,106]. The $[Ru(trpy)(3,5\text{-}^tBu_2C_6H_2O_2)(OH_2)]^{2+}$ complex was initially assigned as Ru^{III}–NIL•, however, subsequent theoretical analysis by Muckerman et al. indicated a predominant Ru^{II}–NIL^{Ox} character with a noteworthy contribution from the Ru^{III}–NIL• resonance form. This electronic structure is consistent with a large portion of Class B complexes covered in this review [21]. The crystal structure displays a C_1–C_2 distance of 1.466 Å along with C_1–O_1 and C_2–O_2 distances of 1.293(5) and 1.280(5) Å, respectively. Ru–O_{NIL} bond lengths of 1.968(3) and 2.028(3) Å were reported with a Ru–O_{aq} bond length of 2.099(3) Å (Fig. 7).[6]

The unusual pH dependence of charge migration within the $[Ru^{II}(trpy)(NIL^{Ox})(OH_2)]^{2+}$ complex was monitored via UV–vis spectroscopy (Fig. 8, Scheme 8) [106]. Deprotonation of the $[Ru^{II}(trpy)(NIL^{Ox})(OH_2)]^{2+}$ compound ($pK_a = 5.5$) forms the $[Ru^{II}(trpy)(NIL^{Ox})(OH)]^+$ species. This reaction is accompanied by a slight blue shift of the MLCT transition from 600 nm to 576 nm (Fig. 8a–d). The second deprotonation ($pK_a = 10.7$) affords the

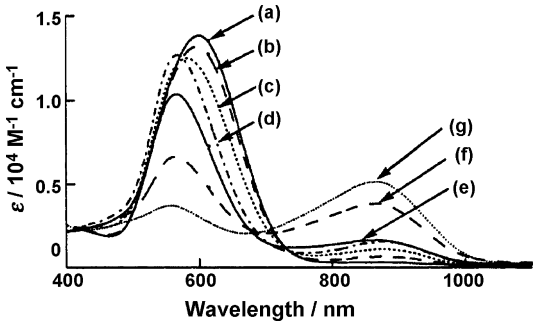

Fig. 8. The pH titration of $[Ru(trpy)(3,5\text{-}^tBu_2C_6H_2O_2)(OH_2)]^{2+}$: (a) pH 3.2; (b) pH 4.5; (c) pH 5.6; (d) pH 7.1; (e) pH 10.1; (f) pH 11.0; (g) pH 12.0. This figure was reproduced from Ref. [106].

highly reactive $[Ru^{II}(trpy)(NIL•)(O•^-)]^0$ species which rapidly undergoes H-atom abstraction to give $[Ru^{II}(trpy)(NIL•)(OH)]^0$. The conversion of $[Ru^{II}(trpy)(NIL^{Ox})(OH)]^+$ to $[Ru^{II}(trpy)(NIL•)(OH)]^0$ is indicated by a dramatic red shift in the MLCT[4] band from 576 to 870 nm (Fig. 8d and e), consistent with previous reports by Lever for isoelectronic species [86].[7] The highly reactive $[Ru^{II}(trpy)(NIL•)(O•^-)]^0$ species (Scheme 8, iii) is plausible due to the strong acceptor character of the NIL ligand in the ruthenium oxo species – in fact, the Ru(=O) species is unfavorable here due to the full Ru^{II} t_{2g} valence shell [21]. A crystal structure of "$[Ru^{II}(trpy)(NIL•)(O•^-)]^0$" has been reported by Kobayashi et al., however, it is likely the H-atom abstraction species $[Ru^{II}(trpy)(NIL•)(OH)]^0$ with the hydroxyl proton elusive to detection by X-ray diffraction [21,106]. Although highly reactive, the oxyl radical species was detected by a spin trapping EPR experiment using 5,5-dimethyl-1-pyrroline *N*-oxide (DMPO) with an observed 12-line signal centered at $g = 2.006$ [105,106]. Treatment of $[Ru^{II}(trpy)(NIL•)(OH)]^0$ with acid in air regenerates the starting aqua complex $[Ru^{II}(trpy)(NIL^{Ox})(OH_2)]^{2+}$(Scheme 8).

The cyclic voltammetry of $[Ru(trpy)(3,5\text{-}^tBu_2C_6H_2O_2)(OH_2)]^{2+}$ was investigated in the presence of base (Fig. 9) [105–107]. Upon addition of a slight excess of ^{t}BuOK to $[Ru(trpy)(3,5\text{-}^tBu_2C_6H_2O_2)(OH_2)]^{2+}$, a progression from the Class B species $[Ru^{II}(trpy)(NIL^{Ox})(OH_2)]^{2+}$ (which displays two reduction events at 0.31 and −0.47 V *vs.* SCE; $V_{rest} = 0.48$ V), to the Class B species $[Ru^{II}(trpy)(NIL^{Ox})(OH)]^+$ (which displays an oxidation event at 0.07 V and a reduction event at −0.57 V *vs.* SCE; $V_{rest} = 0.36$ V) is detected. Additional base results in the formation of the Class C species $[Ru^{II}(trpy)(NIL•)(O•^-)]^0$ which is highly reactive and abstracts a proton to form $[Ru^{II}(trpy)(NIL•)(OH)]^0$ (which displays one oxidation event at 0.31 V and one reduction event at −0.47 V *vs.* SCE; $V_{rest} = 0.17$ V), the rest potential shifting cathodically across the first redox couple (Scheme 8). The pH dependent shift of V_{rest} for $[Ru(trpy)(3,5\text{-}^tBu_2C_6H_2O_2)(OH_2)]^{2+}$ has been exploited by Tsuge et al. for the generation of electrical current in a two compartment electrolytic cell [105,107]. Now we start to see how the reactivity of Ru–NIL species can be dictated by the synergistic Ru(dπ)–NIL(π*) and Ru(dπ)–NIL(π) bonding interactions discussed earlier.

Until recently it was assumed that molecular water oxidation catalysts required at least two high-valent transition metal centers in close proximity with the appropriate stereochemistry for O_2 bond formation [108,109]. Although deprotonation of $[Ru(trpy)(3,5\text{-}^tBu_2C_6H_2O_2)(OH_2)]^{2+}$ affords a highly reactive oxyl radical species, O_2 formation was never observed due to hydrogen atom abstraction (Scheme 8). In contrast, the Tanaka catalyst $[Ru_2(btpyan)(3,6\text{-}^tBu_2C_6H_2O_2)_2(OH)_2]^{2+}$ achieves efficient water

[6] Kobayashi et al. assigned this complex as Ru^{III}NIL•, however, further investigation by Tsai et al. has proven it to be predominantly $Ru^{II}NIL^{Ox}$ with some contribution from the Ru^{III}NIL• configuration, an assignment consistent with XPS data [39,106].

[7] The reduced intensity of the low energy transition from $[Ru^{II}(NIL•)(OH)]^0$ in Fig. 8(a–g) is due to the low solubility of this neutral species at high pH.

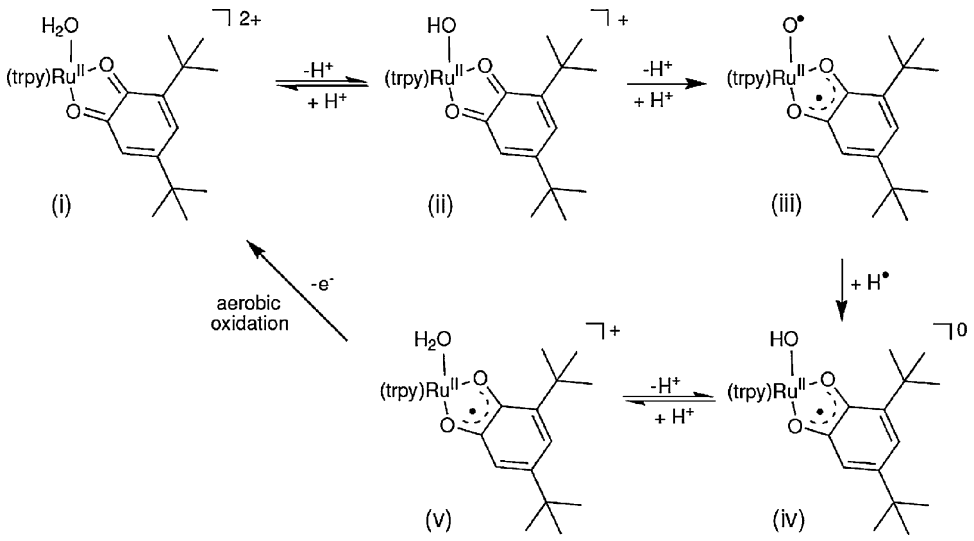

Scheme 8. The pH dependent chemistry of $[Ru(trpy)(3,5\text{-}^tBu_2C_6H_2O_2)(OH_2)]^{2+}$ observed in both organic and aqueous media under aerobic conditions. The reversibility of the pH titration is accounted for by the aerobic oxidation of (v) to (i).

oxidation catalysis, albeit heterogeneously on a tin-doped indium oxide (ITO) electrode [21–23,110]. The dissociation of two protons from the Tanaka catalyst under very basic conditions (2 equivalents ^{t}BuOK in methanol solution) produces a species in which the charge has migrated from the precursor hydroxy ligand to the NIL^{Ox} ligand as evidenced by the disappearance of the Ru^{II}–NIL^{Ox} absorption band at 576 nm and the appearance of new lower-energy transition Ru^{II}–$NIL^{\bullet}$ at 850 nm [22,23,110]. Tentatively the authors suggest that O–O bond formation occurs upon this double deprotonation resulting in the $[Ru^{II}{}_2(btpyan)(NIL^{\bullet})_2(O_2{}^{2-})]^0$ configuration.

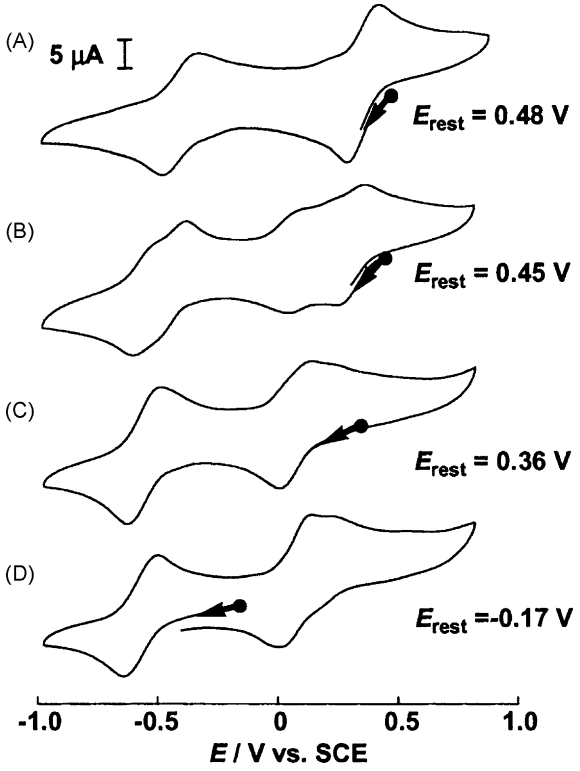

Fig. 9. Cyclic voltammograms of $[Ru(trpy)(3,5\text{-}^tBu_2C_6H_2O_2)(OH_2)]^{2+}$ in CH_2Cl_2 monitoring the progression from $[Ru(trpy)(NIL)(OH_2)]^{2+}$ to $[Ru(trpy)(NIL)(OH)]^+$ to $[Ru(trpy)(NIL)(OH)]^0$ upon addition of: (A) 0; (B) 0.5; (C) 1.0; (D) 3.0 equivalents of ^{t}BuOK in CH_2Cl_2 (0.1 M Bu_4NClO_4). This figure was reproduced from Ref. [106] with permission of the copyright holders.

Evolution of O_2, however, is only observed upon application of a positive potential, where in acidic conditions, i.e., pH 4, deprotonation takes place via a proton-coupled electron-transfer mechanism [21,39]. The Tanaka catalyst displays four quasi-reversible redox couples negative of its rest potential (+0.49 V *vs.* Ag/AgCl) at +0.43, +0.35, −0.47 and −0.56 V *vs.* Ag/AgCl in methanol attributed to four successive one-electron ligand-based reductions from $[Ru^{II}{}_2(btpyan)(NIL^{Ox})_2(OH)_2]^{2+}$ to $[Ru^{II}{}_2(btpyan)(NIL^{Ox})(NIL^{\bullet})(OH)_2]^+$ to $[Ru^{II}{}_2(btpyan)(NIL^{\bullet})_2(OH)_2]^0$ to $[Ru^{II}{}_2(btpyan)(NIL^{Red})(NIL^{\bullet})(OH)_2]^-$ to $[Ru^{II}{}_2(btpyan)(NIL^{Red})_2(OH)_2]^{2-}$ indicating a communication between the two NIL ligands across the two metal centers [22]. Methanol and acetone solvents both undergo oxidation at potentials >+1.00 V *vs.* Ag/AgCl in the presence of the Tanaka catalyst, precluding observation of any redox chemistry at more positive potentials. The $Ru^{III/II}$ couple was observed at +1.34 V *vs.* Ag/AgCl for both metal centers via a two-electron redox process in a 1:1 mixture of trifluoroethanol and ether thus forming $[Ru^{III}{}_2(btpyan)(NIL^{Ox})_2(OH)_2]^{4+}$.

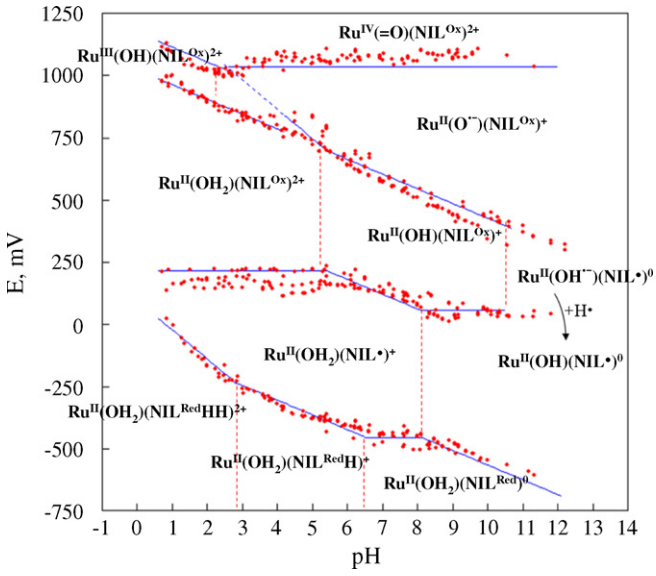

Fig. 10. A Pourbaix diagram of $[Ru(trpy)(3,5\text{-}^tBu_2C_6H_2O_2)(OH_2)]^{2+}$. Potential is given relative to the SCE. This figure was reproduced from ref. [39] with permission of the copyright holders.

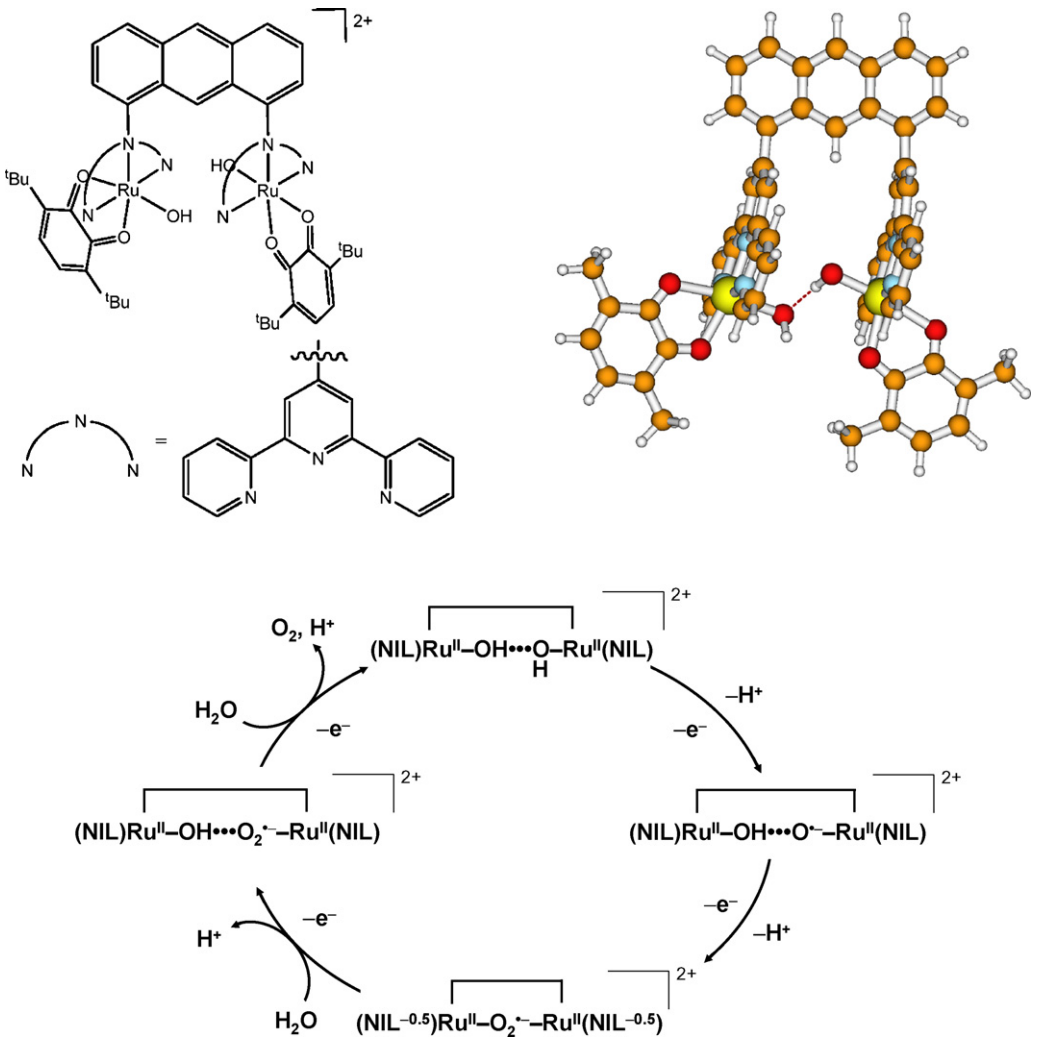

Scheme 9. A schematic of the Tanaka catalyst (top left) and the calculated RIMP2 geometric structure for the Me (instead of ^{t}Bu) substituted species (top right). The proposed catalytic cycle for water oxidation by the Tanaka catalyst in aqueous solution at pH 4 (bottom).

Controlled-potential electrolysis of the Tanaka catalyst at 1.70 V *vs.* Ag/AgCl in trifluoroethanol containing 10% water evolves O_2 with a current efficiency >90% with a turnover number (TN) of 21 [22]. When the catalyst is physisorbed onto ITO in water at pH 4, the $Ru^{III/II}$ redox couple occurs at 1.19 V *vs.* Ag/AgCl and is proton coupled [21,22,39], forming the fully deprotonated species $[Ru^{II}{}_2(btpyan)(NIL^{-0.5})_2(O)_2]^{2+}$ which is believed to be the O–O bond formation step for water oxidation [21,22,39]. At pH 4, with a controlled potential electrolysis at +1.70 V *vs.* Ag/AgCl, a turnover number > 30,000 was recorded over a 40 h period – the highest reported turnover number to date for a molecular catalyst for water oxidation.[8] In fact, the catalyst is still intact after 40 h but the current gradually decreases as the pH decreases and the physisorbed catalyst falls off the electrode.

The Pourbaix diagram, i.e., pH dependent voltammetry, of the monomer complex $[Ru(trpy)(3,5\text{-}^{t}Bu_2C_6H_2O_2)(OH_2)]^{2+}$ reported by Tsai et al. is a perfect illustration of the complex redox chemistry observed for these systems (Fig. 10) [39]. Formation of the oxyl radical species $[Ru^{II}(trpy)(NIL^{Ox})(O^{\bullet -})]^{+}$ is observed via two-proton, one-electron-coupled oxidation of $[Ru(trpy)(3,5\text{-}^{t}Bu_2C_6H_2O_2)(OH_2)]^{2+}$ as evidenced by a slope of −118 mV/pH in the pH regions 3–6. There is a lot of scatter related to these data points which has been attributed to H-atom abstraction by the oxyl radical species forming $[Ru(trpy)(3,5\text{-}^{t}Bu_2C_6H_2O_2)(OH)]^{+}$ that is subsequently protonated to regenerate $[Ru(trpy)(3,5\text{-}^{t}Bu_2C_6H_2O_2)(OH_2)]^{2+}$. It should be mentioned that this plot was reproduced theoretically (with nearly complete topological accuracy, but with expanded scales on both axes), taking into consideration the various geometry optimizations and spin multiplicities for all species involved to aid in their assignment. Although the monomer species does not show any catalytic activity for water oxidation reaction, its investigation has certainly shed some light on the redox chemistry of the Tanaka catalyst.

The mechanism for O_2 evolution was investigated by Muckerman et al. [21,22,39] using a combination of theoretical and experimental techniques (Scheme 9). Interestingly, all redox chemistry occurred either at the aqua moieties or the NIL. Unlike other molecular water oxidation catalysts, the Ru centers remain low valent and appear to play an active role by facilitating the charge migration from the aqua ligand to the NIL^{Ox} moieties. This charge

[8] An applied potential of 1.70 V *vs.* Ag/AgCl at pH 4 represents an overpotential of 0.90 V for the oxidation of water (E° = 0.62 V *vs.* Ag/AgCl at pH 7; ±0.059 V/pH). Although this appears as quite a large overpotential, the onset potential for the observance of catalytic current occurs at 1.19 V *vs.* Ag/AgCl representing an overpotential of just 0.41 V.

migration is made possible by the extensive electron delocalization throughout the Ru(dπ)–NIL(π*) framework.

Electrochemical analysis of the $[Ru_2(btpyan)(3,5\text{-}Cl_2C_6H_2O_2)_2(OH)_2]^{2+}$ and $[Ru_2(btpyan)(4\text{-}NO_2C_6H_3O_2)_2(OH)_2]^{2+}$ analogs of the Tanaka catalyst displayed no catalytic current for water oxidation under identical conditions or even at applied potentials up to 2.00 V *vs.* Ag/AgCl. This was explained by an anodic shift of the NIL and Ru redox couples due to the electron withdrawing effect of the NIL substituents, and a failure to advance to the second deprotonation step [21].

6. Conclusion

This review examined a wide variety of Ru–NIL complexes and their respective electron distributions. The electron distributions within the Ru–NIL fragments are sensitive to substituent effects on the NIL and the choice of ancillary ligands. Thus the electronic structure of a system can be "tuned" by manipulating the mixing between the low-lying π* ligand orbitals of the NIL and the ruthenium dπ orbital. Due to the extensive mixing of the Ru and NIL orbitals in these complexes, the ruthenium centers and NIL possess non-integer oxidation states in certain systems. The oxidation-state assignments in these cases, especially for Class B systems, are non-trivial and can easily be misassigned. To accurately assign electron distributions in these systems, one must evaluate a series of spectroscopic, electrochemical, and structural data together with predictions from careful theoretical analyses.

The Class B systems of the generic formula $[Ru(trpy)(NIL)X]^+$ ($[Ru(trpy)(C_6H_4NHNH)(Cl)]^+$, $[Ru(trpy)(C_6H_4ONH)(OAc)]^+$, $[Ru(trpy)(3,5\text{-}^tBu_2C_6H_2O_2)(NH_2)]^+$ and $[Ru(trpy)(3,5\text{-}^tBu_2C_6H_2O_2)(OH)]^+$) exhibit non-integer oxidation states for the metal and NIL with a particular Ru oxidation state displaying a predominate contribution. In these systems the electron distribution is delocalized not only over the Ru–NIL fragments but also the X ligand trans to the NIL. The utility of this Class B $[Ru(trpy)(NIL)X]^+$ motif has been demonstrated in the $[Ru_2(btpyan)(NIL)_2(OH)_2]^{2+}$ and $[Ru(trpy)(3,5\text{-}^tBu_2C_6H_2O_2)(NH_3)]^{2+}$ systems. These Ru–NIL ensembles catalyze the sophisticated redox reactions of water oxidation and alcohol oxidation, respectively. This ability to spread electrons over the framework enables the Ru–NIL's fragments to act as electron reservoirs and help stabilize reactive radical intermediates, all while avoiding a high valent metal center in these catalytic reactions.

Acknowledgement

Work performed at Brookhaven National Laboratory was funded under contract DE-AC02-98CH10886 with the U.S. Department of Energy and supported by its Division of Chemical Sciences, Geosciences, and Biosciences, Office of Basic Energy Sciences.

Appendix. Two-electron, two-orbital model for understanding the electronic structure of Class B Ru–NIL complexes

We will begin by describing the "infinite separation" (no overlap) valence bond (VB) states of a model of Class B Ru–NIL complexes involving two electrons and two orbitals. These are the appropriate states for describing the formal oxidation states of their Ru and NIL constituents even though they are inconvenient basis states for carrying out actual calculations on the Ru–NIL complex. A similar two-electron, two-orbital analysis has been carried out by Nocera for the very different case of δ^2 configurations in quadruple-bonded metal-metal complexes to explain their two-photon spectroscopy [111].

Let us assume that the Ru constituent of the complex has a four-coordinate, closed-shell Ru(IV) core with one valence orbital, the unoccupied dπ orbital among its "t_{2g}" orbitals, and let the NIL ligand have a closed-shell NIL^{Ox} core with one valence orbital, the lowest π* orbital of the NIL π system. These two valence orbitals will be designated as *a* and *b*, respectively. We will here address the Class B case of complexes for which we will construct electronic states by assigning two electrons to these two localized orbitals in all possible ways. In so doing, we will be constructing VB basis states because we will be approximating the electronic eigenstates of the system by linear combinations of products of fragment orbitals rather than, as in the MO approach, products of linear combinations of fragment orbitals.

If we assign both electrons to a single fragment orbital, we will obtain a closed-shell VB basis state. In the case of assigning both electrons to the Ru atom, we obtain a closed-shell VB basis state (CS1) corresponding to Ru^{II}-NIL^{Ox},

$$^1\Psi_{CS1} = |a\bar{a}|.$$

Here we designate a VB basis state with the symbol Ψ and use the notation of the Slater determinant, where for any two orbitals *c* and *d*,

$$|c\bar{d}| \equiv \frac{1}{\sqrt{2}} \begin{vmatrix} c(1) & \bar{d}(1) \\ c(2) & \bar{d}(2) \end{vmatrix},$$

with the bar over an orbital indicating that the electron in it has beta spin (the absence of a bar indicating alpha spin). If both electrons are assigned to the NIL fragment, we obtain the closed-shell VB basis state (CS2) corresponding to the Ru^{IV}–NIL^{Red} complex,

$$^1\Psi_{CS2} = |b\bar{b}|$$

Note that both these closed-shell VB basis states necessarily have $M_S = 0$ ($m_S = +(1/2)$ for the alpha-spin electron and $m_S = -(1/2)$ for the beta-spin electron) because they correspond to singlet states with $S = 0$. When we assign one electron to each of the two fragments to make basis states corresponding to Ru^{III}–$NIL^{\bullet}$, things become more complicated because an open-shell singlet state cannot be described by a single determinant (nor can the $M_S = 0$ component of a triplet state). The open-shell singlet VB basis state (OS) is

$$^1\Psi_{OS} = \frac{1}{\sqrt{2(1+s^2)}}\{|a\bar{b}| - |\bar{a}b|\},$$

where *s* is the overlap integral between orbitals *a* and *b*, and the same two determinants can be used to describe the $M_S = 0$ component of the VB triplet state,

$$^3\Psi_{OS} = \frac{1}{\sqrt{2(1-s^2)}}\{|a\bar{b}| + |\bar{a}b|\}.$$

These VB states, three singlets and one triplet, can be used as a basis for approximating the corresponding electronic eigenstates of the Ru–NIL complex. In some cases, one of the basis states will be dominant, in other cases more than one of the basis states will be important, and we refer to the latter case as "resonance", which is another VB concept. Note that $^1\Psi_{OS}$ corresponds to a "singlet biradical" description of the electronic structure because one electron is on each fragment.

Another complication with the VB approach is that the VB basis states do not remain orthogonal as the fragments are moved from infinite separation (i.e., non-interacting) to finite separation because of the overlap of orbitals *a* and *b*. The overlap matrix of our

VB basis of three singlet states and one triplet state is

$$\mathbf{S} = \begin{bmatrix} 1 & s^2 & \frac{2s}{\sqrt{2(1+s^2)}} & 0 \\ s^2 & 1 & \frac{2s}{\sqrt{2(1+s^2)}} & 0 \\ \frac{2s}{\sqrt{2(1+s^2)}} & \frac{2s}{\sqrt{2(1+s^2)}} & 1 & 0 \\ 0 & 0 & 0 & 1 \end{bmatrix},$$

which immediately reveals that while the three singlet VB states remain orthogonal to the VB triplet state, they do not remain orthogonal to each other. This results in the partial breakdown of all the VB-based logical constructs that apply only to the infinite separation (no overlap) case. Among these are the distinction between ionic and covalent states, the distinction between closed and open shells, and (especially) the definition of formal oxidation states.

Now let us start again, but this time describe the same two-orbital, two-electron model in terms of the MO picture. This begins by constructing molecular orbitals as linear combinations of the fragment orbitals,

$$\varphi = \frac{1}{\sqrt{2(1+s)}}(a+b), \quad \pi \text{ bonding MO}$$

and

$$\varphi* = \frac{1}{\sqrt{2(1-s)}}(a-b), \quad \pi \text{ antibonding MO}.$$

Here we have assumed that the orbitals a and b are quasi-degenerate so that we can specify their linear combination by inspection rather than by performing a variational calculation. This will often be a good approximation for the Class B Ru–NIL complexes. These molecular orbitals are orthogonal by construction. We can now build MO basis states by assigning the electrons to these molecular orbitals and constructing products of the occupied orbitals. If we assign both electrons to the π-bonding MO, the so-called $(\pi)^2$ configuration, we obtain an approximation to the electronic ground-state wavefunction (the so-called principal configuration wavefunction),

$$\begin{aligned} {}^1\Phi_{CS1} &= |\varphi\bar{\varphi}| = \tfrac{1}{2(1+s)}\{|a\bar{a}| + |a\bar{b}| - |\bar{a}b| + |b\bar{b}|\} \\ &= \tfrac{1}{2(1+s)}\{{}^1\Psi_{CS1} + {}^1\Psi_{CS2} + \sqrt{2(1+s^2)}\,{}^1\Psi_{OS}\} \end{aligned}$$

Here we designate a MO basis state with the symbol Φ, and have substituted the expression for the MO φ in terms of orbitals a and b, expanded the products, and then collected terms to project onto the VB basis states. If we assign both electrons to the π-antibonding MO, the $(\pi^*)^2$ configuration, we obtain

$$\begin{aligned} {}^1\Phi_{CS2} &= |\varphi*\bar{\varphi}*| = \tfrac{1}{2(1-s)}\{|a\bar{a}| - (|a\bar{b}| - |\bar{a}b|) + |b\bar{b}|\} \\ &= \tfrac{1}{2(1-s)}\{{}^1\Psi_{CS1} + {}^1\Psi_{CS2} - \sqrt{2(1+s^2)}\,{}^1\Psi_{OS}\} \end{aligned}$$

which is a different linear combination of the three singlet VB basis states contained in ${}^1\Phi_{CS1}$.

We could now construct the open-shell singlet and triplet MO states by analogy with the open-shell VB states, but it is instructive to build the constituent Slater determinants in terms of the molecular orbitals. These are

$$\begin{aligned} |\varphi\bar{\varphi}*| &= \tfrac{1}{2\sqrt{1-s^2}}\{|a\bar{a}| - (|a\bar{b}| + |\bar{a}b|) - |b\bar{b}|\} \\ &= \tfrac{1}{2\sqrt{1-s^2}}\{{}^1\Psi_{CS1} - {}^1\Psi_{CS2}\} - \tfrac{1}{\sqrt{2}}{}^3\Psi_{OS} \end{aligned}$$

and

$$\begin{aligned} |\bar{\varphi}\varphi*| &= \tfrac{1}{2\sqrt{1-s^2}}\{-|a\bar{a}| + (|a\bar{b}| + |\bar{a}b|) + |b\bar{b}|\} \\ &= \tfrac{1}{2\sqrt{1-s^2}}\{-{}^1\Psi_{CS1} + {}^1\Psi_{CS2}\} - \tfrac{1}{\sqrt{2}}{}^3\Psi_{OS} \end{aligned}$$

which can be seen to be impure spin states because each is a mixture of singlet and triplet states. The appropriate linear combinations of these two determinants to obtain pure spin states are

$${}^1\Phi_{OS} = \tfrac{1}{\sqrt{2}}\{|\varphi\bar{\varphi}*| - |\bar{\varphi}\varphi*|\} = \tfrac{1}{\sqrt{2(1-s^2)}}\{{}^1\Psi_{CS1} - {}^1\Psi_{CS2}\}$$

and

$${}^3\Phi_{OS} = \tfrac{1}{\sqrt{2}}\{|\varphi\bar{\varphi}*| + |\bar{\varphi}\varphi*|\} = -{}^3\Psi_{OS}.$$

As there is only one triplet state, it is necessarily the same state in both the VB and MO pictures (the overall sign of the wavefunction is arbitrary), but it can immediately be seen that there is not a one-to-one correspondence between the MO and the VB singlet states; all three VB singlet states are contained in the two closed-shell MO states, and *the open-shell MO state projects only on the two closed-shell VB states*. This leads to the counter-intuitive result that there is no singlet biradical character in ${}^1\Phi_{OS}$ even though it has the same $(\pi)^1(\pi^*)^1$ electronic configuration as the MO triplet state, and that state is a triplet biradical. It is also true that ${}^1\Phi_{OS}$ will necessarily be higher in energy than ${}^3\Phi_{OS}$ if $s \neq 0$ because of the orthogonality of the MOs. This result does not (in itself) rule out the possibility of a singlet biradical electronic ground state because ${}^1\Phi_{OS}$ does not correspond to ${}^1\Psi_{OS}$.

What MO state does correspond to the VB singlet biradical state? This discussion has alluded to "basis states" in both the VB and MO sense, and even "resonance" in the VB sense, but has so far skirted the issue of "configuration interaction" (CI), which is often a necessary tool to obtain an accurate approximation to the true electronic ground-state wavefunction and energy. In the configuration interaction approach, the trial wavefunction is expanded as a linear combination of the basis states, and the variational principle is employed to minimize the electronic energy by varying the expansion coefficients. In the VB approach, this is the quantitative implementation of the concept of resonance. In the MO approach, the level of CI can vary from the inclusion of a few key electronic configurations to "full-CI" that includes all possible configurations for a given basis. Open-shell character in fragments is generated through the inclusion of configurations in which a pair of electrons is excited from a bonding orbital to its corresponding antibonding orbital. This type of CI is known as the "generalized valence bond" approach, or GVB-CI.

If we construct a GVB-CI wavefunction for the case of our Ru–NIL model, we obtain

$${}^1\Phi_{GVB} = \sqrt{1-\gamma^2}|\varphi\bar{\varphi}| + \gamma|\varphi*\bar{\varphi}*|$$

where γ is a parameter that is determined by minimizing the electronic energy of the GVB state. If the variational procedure happens to specify $\gamma = -1/\sqrt{2}$, then

$$\begin{aligned} {}^1\Phi_{GVB} &= \tfrac{1}{\sqrt{2}}\{|\varphi\bar{\varphi}| - |\varphi*\bar{\varphi}*|\} \\ &= \tfrac{1}{\sqrt{2}}\left\{-\tfrac{s}{1-s^2}({}^1\Psi_{CS1} - {}^1\Psi_{CS2}) + \sqrt{\tfrac{2}{1-s^2}}\,{}^1\Psi_{OS}\right\} \end{aligned}$$

which in the limit of $s \to 0$ gives

$${}^1\Phi_{GVB} = {}^1\Psi_{OS}.$$

Thus, we see that the MO description of a singlet biradical state is through the GVB-CI state that happens to have coefficients of ${}^1\Phi_{CS1}$ and ${}^1\Phi_{CS2}$ of equal magnitude. While this commonly occurs when a bond is being dissociated to open-shell fragments, the dividing line between dominant closed-shell and dominant open-shell character is somewhat arbitrary. Clearly, if the percentage of ${}^1\Phi_{CS2}$ in the GVB-CI wavefunction of a complex is somewhere between 25% and the limiting 50%, there is ample justification in designating it as a singlet biradical.

It should be noted that the so-called "anti-ferromagnetically coupled" biradical state that is sometimes obtained in a broken-symmetry (BS) DFT calculations corresponds closely to a GVB-CI state except that it is not a proper spin state. In the present case, the BS state would first be approximated using the fragment-localized orbitals a and b in a trial MO wavefunction by

$$\Psi_{\mathrm{BS}}^{\mathrm{trial}} = |a\bar{b}|$$

and then variationally optimized. The result would be a "state" based on two new orbitals, c and d, which are linear combinations of orbitals a and b,

$$\Psi_{\mathrm{BS}} = |c\bar{d}| = \sqrt{\frac{1+s^2}{2}}\,{}^1\Psi_{\mathrm{OS}} + \sqrt{\frac{1-s^2}{2}}\,{}^3\Psi_{\mathrm{OS}}.$$

Because DFT is intrinsically a single-configuration method, the BS approach must sacrifice the accurate description of the spin state in order to optimize the spatial part of the wavefunction. This approach, owing to the inclusion of electron correlation through a correlation functional, can often yield the most accurate approximation that is practical to the true electronic energy of the system, but because it is a single-configuration method that starts with a biradical wavefunction, it assigns all states for which the BS energy is lower than the high-spin (in the present case, triplet) energy as an anti-ferromagnetically coupled biradical state. This is often not the correct assignment, especially when the orbitals c and d collapse to or closely approach the orbital φ of the closed-shell singlet MO state ${}^1\Phi_{\mathrm{CS1}}$ (causing the contribution of the triplet state to vanish or become significantly reduced).

In a complete active space, self-consistent field (CASSCF) calculation on a Class B Ru–NIL complex, one generally employs an active space larger than that of two electrons in two orbitals, but nevertheless there are usually only a few of the many possible configurations that are important (i.e., have non-negligible expansion coefficients). The most common are of the GVB-CI type, but sometimes open-shell MO configurations are also important. We conclude this appendix with the identification of a "footprint" of important CASSCF MO configurations for each of the singlet VB basis states. (It should be reemphasized that the three singlet VB states, ${}^1\Psi_{\mathrm{CS1}}$, ${}^1\Psi_{\mathrm{CS2}}$ and ${}^1\Psi_{\mathrm{OS}}$, correspond to the three singlet resonance structures in the Class B column of Scheme 2.) This is accomplished by inverting the transformations derived above for expressing the MO configurations in terms of the VB basis states. This gives

$$\begin{bmatrix} {}^1\Psi_{\mathrm{CS1}} \\ {}^1\Psi_{\mathrm{CS2}} \\ {}^1\Psi_{\mathrm{OS}} \end{bmatrix} = \begin{bmatrix} \frac{1+s}{2} & \frac{1-s}{2} & \frac{\sqrt{2(1-s^2)}}{2} \\ \frac{1+s}{2} & \frac{1-s}{2} & -\frac{\sqrt{2(1-s^2)}}{2} \\ \frac{1+s}{\sqrt{2(1+s^2)}} & -\frac{1-s}{\sqrt{2(1+s^2)}} & 0 \end{bmatrix} \begin{bmatrix} {}^1\Phi_{\mathrm{CS1}} \\ {}^1\Phi_{\mathrm{CS2}} \\ {}^1\Phi_{\mathrm{OS}} \end{bmatrix},$$

which in the limit of $s \to 0$ becomes

$$\begin{bmatrix} {}^1\Psi_{\mathrm{CS1}} \\ {}^1\Psi_{\mathrm{CS2}} \\ {}^1\Psi_{\mathrm{OS}} \end{bmatrix} = \begin{bmatrix} \frac{1}{2} & \frac{1}{2} & \frac{1}{\sqrt{2}} \\ \frac{1}{2} & \frac{1}{2} & -\frac{1}{\sqrt{2}} \\ \frac{1}{\sqrt{2}} & -\frac{1}{\sqrt{2}} & 0 \end{bmatrix} \begin{bmatrix} {}^1\Phi_{\mathrm{CS1}} \\ {}^1\Phi_{\mathrm{CS2}} \\ {}^1\Phi_{\mathrm{OS}} \end{bmatrix}.$$

The 3×3 $s = 0$ transformation matrix is symmetric and self-adjoint, so it is its own inverse, and defines the transformation in either direction, i.e.,

$$\begin{bmatrix} {}^1\Phi_{\mathrm{CS1}} \\ {}^1\Phi_{\mathrm{CS2}} \\ {}^1\Phi_{\mathrm{OS}} \end{bmatrix} = \begin{bmatrix} \frac{1}{2} & \frac{1}{2} & \frac{1}{\sqrt{2}} \\ \frac{1}{2} & \frac{1}{2} & -\frac{1}{\sqrt{2}} \\ \frac{1}{\sqrt{2}} & -\frac{1}{\sqrt{2}} & 0 \end{bmatrix} \begin{bmatrix} {}^1\Psi_{\mathrm{CS1}} \\ {}^1\Psi_{\mathrm{CS2}} \\ {}^1\Psi_{\mathrm{OS}} \end{bmatrix}.$$

If the fragment orbitals were not degenerate, but orbital a was somewhat lower in energy owing to substituent effects, then this picture changes slightly. If, in the zero-overlap regime, $\varphi = (\sqrt{3}/2)a + (1/2)b$ and $\varphi* = (1/2)a - (\sqrt{3}/2)b$, then the above transformation would more strongly favor $\mathrm{Ru^{II}}$–$\mathrm{NIL^{Ox}}$ in the principal configuration:

$$\begin{bmatrix} {}^1\Phi_{\mathrm{CS1}} \\ {}^1\Phi_{\mathrm{CS2}} \\ {}^1\Phi_{\mathrm{OS}} \end{bmatrix} = \begin{bmatrix} \frac{3}{4} & \frac{1}{4} & \frac{\sqrt{6}}{4} \\ \frac{1}{4} & \frac{3}{4} & -\frac{\sqrt{6}}{4} \\ \frac{\sqrt{6}}{4} & -\frac{\sqrt{6}}{4} & -\frac{\sqrt{2}}{2} \end{bmatrix} \begin{bmatrix} {}^1\Psi_{\mathrm{CS1}} \\ {}^1\Psi_{\mathrm{CS2}} \\ {}^1\Psi_{\mathrm{OS}} \end{bmatrix}.$$

Similarly, if the polarization of the π-bonding MO favored orbital b, e.g., $\varphi = (1/2)a + (\sqrt{3}/2)b$ and $\varphi* = (\sqrt{3}/2)a - (1/2)b$, then the principal configuration would have substantial $\mathrm{Ru^{IV}}$–$\mathrm{NIL^{Red}}$ character.

In summary, we have shown that the principal configuration MO wavefunction is the result of a resonance among all the singlet VB states with significant singlet biradical character, i.e., has significant $\mathrm{Ru^{III}}$–$\mathrm{NIL^{\bullet}}$ character. Valence configuration interaction can shift the balance of this resonance to favor either more $\mathrm{Ru^{II}}$–$\mathrm{NIL^{Ox}}$ or $\mathrm{Ru^{III}}$–$\mathrm{NIL^{\bullet}}$ character, e.g., a GVB-CI with the opposite sign for γ as defined above can diminish or eliminate the $\mathrm{Ru^{III}}$–$\mathrm{NIL^{\bullet}}$ character, and open-shell MO configurations can enhance or diminish $\mathrm{Ru^{IV}}$-$\mathrm{NIL^{Red}}$ character. Non-degeneracy of the Ru dπ and NIL π* orbitals can shift the balance among the resonance structures as well.

References

[1] A.M. Allgeier, C.A. Mirkin, Angew. Chem. Int. Ed. 37 (1998) 895.
[2] P. Chaudhuri, K. Wieghardt, Prog. Inorg. Chem. 50 (2001) 151.
[3] M.R. Haneline, A.F. Heyduk, J. Am. Chem. Soc. 128 (2006) 8410.
[4] K.J. Blackmore, N. Lal, J.W. Ziller, A.F. Heyduk, J. Am. Chem. Soc. 130 (2008) 2728.
[5] M.W. Bouwkamp, A.C. Bowman, E. Lobkovsky, P.J. Chirik, J. Am. Chem. Soc. 128 (2006) 13340.
[6] M.R. Ringenberg, S.L. Kokatam, Z.M. Heiden, T.B. Rauchfuss, J. Am. Chem. Soc. 130 (2008) 788.
[7] G.A. Abakumov, A.I. Poddel'sky, E.V. Grunova, V.K. Cherkasov, G.K. Fukin, Y.A. Kurskii, L.G. Abakumova, Angew. Chem. Int. Ed. 44 (2005) 2767.
[8] J. Stubbe, W.A. van der Donk, Chem. Rev. 98 (1998) 705.
[9] W. Kaim, Dalton Trans. (2003) 761.
[10] N.S. Lewis, D.G. Nocera, Proc. Nat. Acad. Sci. 103 (2006) 15729.
[11] K.N. Ferreira, T.M. Iverson, K. Maghlaoui, J. Barber, S. Iwata, Science 303 (2004) 1831.
[12] J.P. McEvoy, G.W. Brudvig, Chem. Rev. 106 (2006) 4455.
[13] T.J. Meyer, M.H.V. Huynh, H.H. Thorp, Angew. Chem. Int. Ed. 46 (2007) 5284.
[14] C. Tommos, G.T. Babcock, Acc. Chem. Res. 31 (1998) 18.
[15] T.-C. Weng, W.-Y. Hsieh, E.S. Uffelman, S.W. Gordon-Wylie, T.J. Collins, V.L. Pecoraro, J.E. Penner-Hahn, J. Am. Chem. Soc. 126 (2004) 8070.
[16] W. Ruttinger, G.C. Dismukes, Chem. Rev. 97 (1997) 1.
[17] J. Barber, Chem. Soc. Rev. 38 (2009) 185.
[18] V.K. Yachandra, K. Sauer, M.P. Klein, Chem. Rev. 96 (1996) 2927.
[19] S.W. Gersten, G.J. Samuels, T.J. Meyer, J. Am. Chem. Soc. 104 (1982) 4029.
[20] J. Limburg, J.S. Vrettos, L.M. Liable-Sands, A.L. Rheingold, R.H. Crabtree, G.W. Brudvig, Science 283 (1999) 1524.
[21] J.T. Muckerman, D.E. Polyansky, T. Wada, K. Tanaka, E. Fujita, Inorg. Chem. 47 (2008) 1787.
[22] T. Wada, K. Tsuge, K. Tanaka, Inorg. Chem. 40 (2001) 329.
[23] T. Wada, K. Tsuge, K. Tanaka, Angew. Chem. Int. Ed. 39 (2000) 1479.
[24] W. Kaim, Coord. Chem. Rev. 76 (1987) 187.
[25] A.B.P. Lever, H. Masui, R.A. Metcalfe, D.J. Stufkens, E.S. Dodsworth, P.R. Auburn, Coord. Chem. Rev. 125 (1993) 317.
[26] A.I. Poddel'sky, V.K. Cherkasov, G.A. Abakumov, Coord. Chem. Rev. 253 (2009) 291.

[27] P. Zanello, M. Corsini, Coord. Chem. Rev. 250 (2006) 2000.
[28] K.P. Butin, E.K. Beloglazkina, N.V. Zyk, Russ. Chem. Rev. 74 (2005) 531.
[29] C.G. Pierpont, R.M. Buchanan, Coord. Chem. Rev. 38 (1981) 45.
[30] C.G. Pierpont, Coord. Chem. Rev. 216/217 (2001) 99.
[31] E. Evangelio, D. Ruiz-Molina, Eur. J. Inorg. Chem. (2005) 2957.
[32] C.K. Jorgensen, Coord. Chem. Rev. 1 (1966) 164.
[33] S.I. Gorelsky, A.B.P. Lever, M. Ebadi, Coord. Chem. Rev. 230 (2002) 97.
[34] S. Patra, B. Sarkar, S.M. Mobin, W. Kaim, G.K. Lahiri, Inorg. Chem. 42 (2003) 6469.
[35] S. Maji, S. Patra, S. Chakraborty, D. Janardanan, S.M. Mobin, R.B. Sunoj, G.K. Lahiri, Eur. J. Inorg. Chem. (2007) 314.
[36] R.A. Metcalfe, A.B.P. Lever, Inorg. Chem. 36 (1997) 4762.
[37] F.N. Rein, R.C. Rocha, H.E. Toma, Electrochem. Commun. 4 (2002) 436.
[38] S.F. Ye, B. Sarkar, C. Duboc, J. Fiedler, W. Kaim, Inorg. Chem. 44 (2005) 2843.
[39] M.-K. Tsai, J. Rochford, D.E. Polyansky, T. Wada, K. Tanaka, E. Fujita, J.T. Muckerman, Inorg. Chem. 48 (2009) 4372.
[40] C. Remenyi, M. Kaupp, J. Am. Chem. Soc. 127 (2005) 11399.
[41] T. Wada, M. Yamanaka, T. Fujihara, Y. Miyazato, K. Tanaka, Inorg. Chem. 45 (2006) 8887.
[42] R.B. Salmonsen, A. Abelleira, M.J. Clarke, S.D. Pell, Inorg. Chem. 23 (1984) 385.
[43] M.D. Ward, J.A. McCleverty, J. Chem. Soc., Dalton Trans. (2002) 275.
[44] C.G. Pierpont, Coord. Chem. Rev. 219–221 (2001) 415.
[45] S. Ghumaan, B. Sarkar, S. Maji, V.G. Puranik, J. Fiedler, F.A. Urbanos, R. Jimenez-Aparicio, W. Kaim, G.K. Lahiri, Chem. Eur. J. 14 (2008) 10816.
[46] M.R. Churchill, C.H. Lake, W. Paw, J.B. Keister, Organometallics 13 (1994) 8.
[47] D.S. Bohle, A.N. Christensen, P.A. Goodson, Inorg. Chem. 32 (1993) 4173.
[48] M. Kondo, M. Hamatani, S. Kitagawa, J. Am. Chem. Soc. 120 (1998) 455.
[49] S. Takemoto, S. Oshio, T. Shiromoto, H. Matsuzaka, Organometallics 24 (2005) 801.
[50] N. Bag, G.K. Lahiri, P. Basu, A. Chakravorty, J. Chem. Soc., Dalton Trans. (1992) 113.
[51] S. Bhattacharya, C.G. Pierpont, Inorg. Chem. 33 (1994) 6038.
[52] S. Bhattacharya, C.G. Pierpont, Inorg. Chem. 31 (1992) 35.
[53] P.R. Auburn, E.S. Dodsworth, M. Haga, W. Liu, W.A. Nevin, A.B.P. Lever, Inorg. Chem. 30 (1991) 3502.
[54] K. Ray, T. Petrenko, K. Wieghardt, F. Neese, Dalton Trans. (2007) 1552.
[55] H. Masui, Coord. Chem. Rev. 219–221 (2001) 957.
[56] S. Bhattacharya, P. Gupta, F. Basuli, C.G. Pierpont, Inorg. Chem. 41 (2002) 5810.
[57] K. Chłopek, E. Bothe, F. Neese, T. Weyhermuller, K. Wieghardt, Inorg. Chem. 45 (2006) 6298.
[58] A.B.P. Lever, E.S. Dodsworth (Eds.), Inorganic Electronic Structure and Spectroscopy, Wiley, New York, 1999.
[59] A.B.P. Lever, S.I. Gorelsky, Struct. Bonding 107 (2004) 77.
[60] A.B.P. Lever, in: A.B.P. Lever (Ed.), Comprehensive Coordination Chemistry II, Elsevier Ltd., 2004, p. 251.
[61] A. Juris, V. Balzani, F. Barigelletti, S. Campagna, P. Belser, A. von Zelewsky, Coord. Chem. Rev. 84 (1988) 85.
[62] S.I. Gorelsky, E.S. Dodsworth, A.B.P. Lever, A.A. Vlcek, Coord. Chem. Rev. 174 (1998) 469.
[63] A.B.P. Lever, S.I. Gorelsky, Coord. Chem. Rev. 208 (2000) 153.
[64] D.J. Stufkens, T.L. Snoeck, A.B.P. Lever, Inorg. Chem. 27 (1988) 953.
[65] H. Masui, A.B.P. Lever, E.S. Dodsworth, Inorg. Chem. 32 (1993) 258.
[66] H. Masui, A.B.P. Lever, P.R. Auburn, Inorg. Chem. 30 (1991) 2402.
[67] C.G. Pierpont, C.W. Lange, Prog. Inorg. Chem. 41 (1994) 331.
[68] A.Y. Girgis, Y.S. Sohn, A.L. Balch, Inorg. Chem. 14 (1975) 2327.
[69] K.N. Mitra, S. Goswami, S.-M. Peng, Chem. Commun. (1998) 1685.
[70] K.N. Mitra, P. Majumdar, S.-M. Peng, A. Castineiras, S. Goswami, Chem. Commun. (1997) 1267.
[71] A. Saha, C. Das, K.N. Mitra, S.-M. Peng, G.H. Lee, S. Goswami, Polyhedron 21 (2002) 97.
[72] K.N. Mitra, S. Goswami, Inorg. Chem. 36 (1997) 1322.
[73] I. Bhattacharyya, M. Shivakumar, A. Chakravorty, Polyhedron 21 (2002) 2761.
[74] G. Ferrando-Miguel, P. Wu, J.C. Huffman, K.G. Caulton, New J. Chem. 29 (2005) 193.
[75] M.K. Tsai, unpublished work.
[76] S.-Y. Yang, W.-H. Leung, Z. Lin, Organometallics 20 (2001) 3198.
[77] C.J. Adams, J.P.H. Charmant, N.G. Connelly, M. Gill, A. Kantacha, S. Onganusorn, A.G. Orpen, Dalton Trans. (2007) 2283.
[78] A. Anillo, C. Barrio, S. Garcia-Granda, R. Obeso-Rosete, J. Chem. Soc., Dalton Trans. (1993) 1125.
[79] D.S. Bohle, K.T. Carron, A.N. Christensen, P.A. Goodson, A.K. Powell, Organometallics 13 (1994) 1355.
[80] M. Hirano, H. Sato, N. Kurata, N. Komine, S. Komiya, Organometallics 26 (2007) 2005.
[81] N.G. Connelly, I. Manners, J.R.C. Protheroe, M.W. Whiteley, J. Chem. Soc., Dalton Trans. (1984) 2713.
[82] F. Hartl, D.J. Stufkens, A. Vlcek Jr., Inorg. Chem. 31 (1992) 1687.
[83] S. Bhattacharya, C.G. Pierpont, Inorg. Chem. 30 (1991) 1511.
[84] D. Venegas-Yazigi, H. Mirza, A.B.P. Lever, A.J. Lough, J. Costamagna, A. Vegae, R. Latorrea, Acta Crystallogr., Sect. C C56 (2000) E245.
[85] P. Belser, A.V. Zelewsky, M. Zehnder, Inorg. Chem. 20 (1981) 3098.
[86] M. Haga, E.S. Dodsworth, A.B.P. Lever, Inorg. Chem. 25 (1986) 447.
[87] D.J. Gordon, R.F. Fenske, Inorg. Chem. 21 (1982) 2907.
[88] D.J. Gordon, R.F. Fenske, Inorg. Chem. 21 (1982) 2916.
[89] S.M. Carter, A. Sia, M.J. Shaw, A.F. Heyduk, J. Am. Chem. Soc. 130 (2008) 5838.
[90] R.S. da Silva, S.I. Gorelsky, E.S. Dodsworth, E. Tfouni, A.B.P. Lever, J. Chem. Soc., Dalton Trans. (2000) 4078.
[91] R.G. de Lima, M.S.P. Marchesi, M.A.F. de Godoy, A.O. Cassano, A.M. de Oliveira, R.S. da Silva, Int. J. Pharm. 271 (2004) 21.
[92] A.B.P. Lever, S.I. Gorelsky, Opt. Spectra Chem. Bond. Transition Metal Complex. 107 (2004) 77.
[93] C. Costentin, Chem. Rev. 108 (2008) 2145.
[94] F.N. Rein, R.C. Rocha, H.E. Toma, J. Inorg. Biochem. 85 (2001) 155.
[95] R.S. Dasilva, E. Tfouni, A.B.P. Lever, Inorg. Chim. Acta 235 (1995) 427.
[96] T. Fujihara, R. Okamura, K. Tanaka, Chem. Lett. 34 (2005) 1562.
[97] M. Kurihara, S. Daniele, K. Tsuge, H. Sugimoto, K. Tanaka, Bull. Chem. Soc. Jpn. 71 (1998) 867.
[98] S. Bhattacharya, Polyhedron 13 (1994) 451.
[99] N. Gupta, N. Grover, G.A. Neyhart, P. Singh, H.H. Thorp, Inorg. Chem. 32 (1993) 310.
[100] J. Rochford, M.-K. Tsai, D.J. Szalda, J.L. Boyer, J.T. Muckerman, E. Fujita, Inorg. Chem., submitted.
[101] T. Hino, T. Wada, T. Fujihara, K. Tanaka, Chem. Lett. 33 (2004) 1596.
[102] T. Wada, T. Fujihara, M. Tomori, D. Ooyama, K. Tanaka, Bull. Chem. Soc. Jpn. 77 (2004) 741.
[103] Y. Miyazato, T. Wada, J.T. Muckerman, E. Fujita, K. Tanaka, Angew. Chem. Int. Ed. 46 (2007) 5728.
[104] Y. Miyazato, T. Wada, K. Tanaka, Bull. Chem. Soc. Jpn. 79 (2006) 745.
[105] K. Tsuge, M. Kurihara, K. Tanaka, Bull. Chem. Soc. Jpn. 73 (2000) 607.
[106] K. Kobayashi, H. Ohtsu, T. Wada, T. Kato, K. Tanaka, J. Am. Chem. Soc. 125 (2003) 6729.
[107] K. Tsuge, K. Tanaka, Chem. Lett. (1998) 1069.
[108] H.-W. Tseng, R. Zong, J.T. Muckerman, R. Thummel, Inorg. Chem. 47 (2008) 11763.
[109] J.J. Concepcion, J.W. Jurss, J.L. Templeton, T.J. Meyer, J. Am. Chem. Soc. 130 (2008) 16462.
[110] T. Wada, K. Tsuge, K. Tanaka, Chem. Lett. (2000) 910.
[111] D.G. Nocera, Acc. Chem. Res. 28 (1995) 209.
[112] A.L.R. Silva, M.O. Santiago, I.C.N. Diogenes, S.O. Pinheiro, E.E. Castellano, J. Ellena, A.A. Batista, F.B.d. Nascimento, I.S. Moreira, Inorg. Chem. Commun. 8 (2005) 1154.
[113] J. Rusanova, E. Rusanov, S.I. Gorelsky, D. Christendat, R. Popescu, A.A. Farah, R.M. Beaulac, C. Reber, A.B.P. Lever, Inorg. Chem. 45 (2006) 6246.
[114] K.N. Mitra, S. Choudhury, A. Castiñeiras, S. Goswami, J. Chem. Soc., Dalton Trans. (1998) 2901.
[115] D. Venegas-Yazigi, H. Mirza, A.B.P. Lever, A.J. Lough, J. Costamagna, R.N. Latorre, Acta Crystallogr., Sect. C 56 (2000) E281.
[116] T. Justel, J. Bendix, N. Metzler-Nolte, T. Weyhermuller, B. Nuber, K. Wieghardt, Inorg. Chem. 37 (1998) 35.
[117] A. Anillo, S. Garcia-Granda, R. Obeso-Rosete, A. Galindo, A. Ienco, C. Mealli, Inorg. Chim. Acta 350 (2003) 557.
[118] A.K. Das, B. Sarkar, C. Duboc, S. Strobel, J. Fiedler, S. Zalis, G.K. Lahiri, W. Kaim, Angew. Chem. Int. Ed. 48 (2009) 4242.
[119] A. Singh, A. Pramanik, G. Das, B. Mondal, Organometallics 27 (2008) 6403.
[120] S.R. Boone, C.G. Pierpont, Inorg. Chem. 26 (1987) 1769.
[121] R. Okamura, T. Wada, K. Aikawa, T. Nagata, K. Tanaka, Inorg. Chem. 43 (2004) 7210.
[122] H. Sugimoto, K. Tanaka, J. Organomet. Chem. 622 (2001) 280.
[123] R.E. DeSimone, R.S. Drago, J. Am. Chem. Soc. 92 (1970) 2343.
[124] R.E. DeSimone, J. Am. Chem. Soc. 95 (1973) 6238.
[125] L. Pasimeni, M. Brustolon, C. Corvaja, J. Magn. Reson. 21 (1976) 259.
[126] W. Kaim, M. Wanner, A. Knodler, S. Zalis, Inorg. Chim. Acta 337 (2002) 163.
[127] F.N. Rein, R.C. Rocha, H.E. Toma, J. Electroanal. Chem. 494 (2000) 21.
[128] C. Das, K.K. Kamar, A.K. Ghosh, P. Majumdar, C.H. Hung, S. Goswami, New J. Chem. 26 (2002) 1409.
[129] K. Kobayashi, F. Ohtsu, T. Wada, K. Tanaka, Chem. Lett. (2002) 868.
[130] T. Wada, K. Tanaka, Eur. J. Inorg. Chem. (2005) 3832.
[131] K. Yang, J.A. Martin, S.G. Bott, M.G. Richmond, Inorg. Chim. Acta 254 (1997) 19.
[132] R.E. Shepherd, A. Proctor, W.W. Henderson, T.K. Myser, Inorg. Chem. 26 (1987) 2440.
[133] T.R. Weaver, T.J. Meyer, S.A. Adeyemi, G.M.B.P. Eckberg, W.E. Hatfield, E.C. Johnson, R.W. Murray, D. Untereker, J. Am. Chem. Soc. 97 (1975) 3039.